MEMS Resonators for High Frequency Applications

Prof. T.K. Bhattacharyya
Dept. of E&ECE, IIT Kharagpur

E&ECE Department
IIT Kharagpur

Motivation

- **Miniaturization of Radio Frequency Transceivers**

Wireless Phone

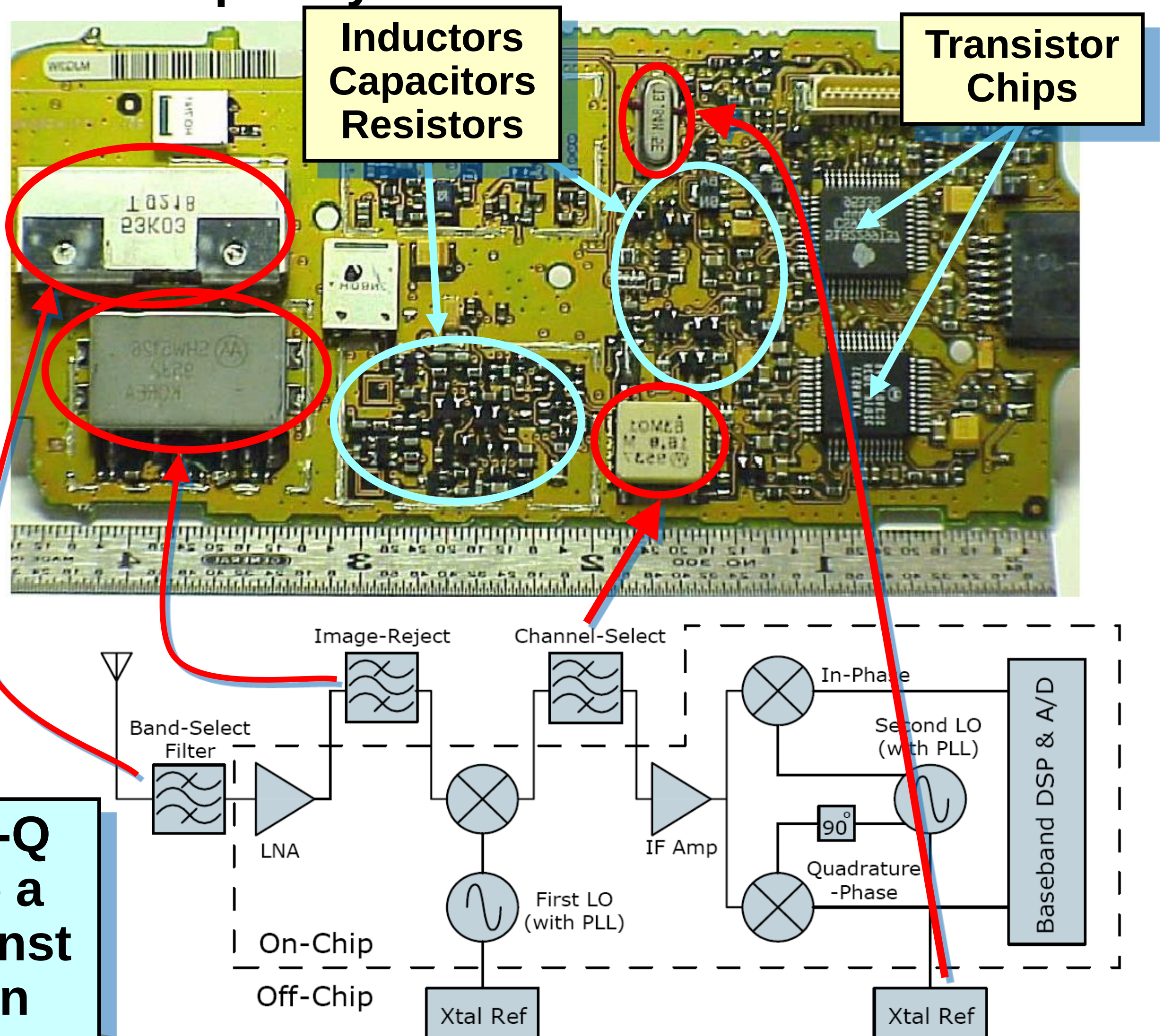

Problem: High-Q passives pose a bottleneck against miniaturization

Source: C. A. Maxey, "Switched-tank VCO designs and single crystal silicon contour-mode disk resonators for use in Multiband Radio Frequency Sources," M. S. Thesis, Virginia Polytechnic Institute and State University, 2004.

Contents

Introduction: Resonators

- **Naturally oscillates at some frequencies (*resonant frequencies*) with greater amplitude than at others**

- **Used to:**
  - **generate signals of precise frequencies**
  - **select specific frequencies from a signal**

- **Key elements in the realization of *filters* and *oscillators***

- **Variants:**
  - **Piezoelectric quartz crystal**
  - **On-chip tank**
  - **Microelectromechanical Resonators**

☑	Large Q
☑	Good temperature stability
☒	Bulky, off-chip
☒	Costly

Micromechanical Resonators: Modes

- **Modes of vibration:**

Micromechanical Resonators: Literature Review

Resonant structure	Material	Dimension(s)	freq.	Q	Schematic diagram
Clamped-clamped beam (flexural mode) Lin et al.(2004)	Poly Silicon (2 µm thick)	Beam length = 40 µm, width = 8 µm	9.34 MHz	3,100	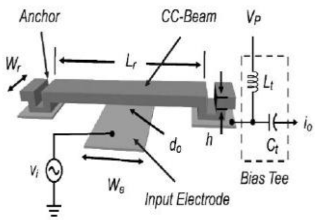
Clamped-clamped beam (flexural mode) Pourkamali et al.(2003)	Single crystal silicon (20 µm thick)	Beam length = 700 µm, width = 6 µm	80 kHz	74,000	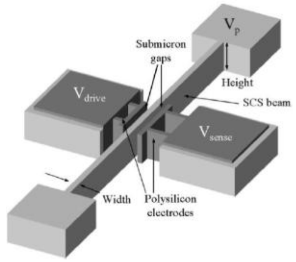
		Beam length = 200 µm, width = 10 µm	3.2 MHz	4,500	
Free-free beam (flexural mode) Wang et al.(2000)	Poly silicon (2.05 µm thick)	Beam length = 13.1 µm, width = 6 µm. Supporting beam length = 10.3 µm, width = 1 µm	92 MHz	7,450	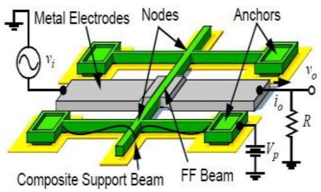
Comb drive (flexural mode) Cioffi and Hsu (2005)	Single crystal silicon (30 µm thick)	No. of comb fingers = 500, finger length = 10 µm, finger overlap = 4 µm	32 kHz	50,000	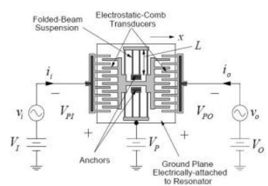

Micromechanical Resonators: Literature Review

Square-plate extensional (bulk acoustic mode) Lee et al.(2008)	Single crystal silicon (25 µm thick)	Side length = 2 mm	2.18 MHz	1,160,000	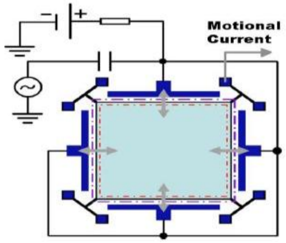
Square plate Lame (bulk) Bhave et al.(2005)	Poly silicon carbide (2 µm thick)	Side length ≈ 35 µm	173 MHz	9,300	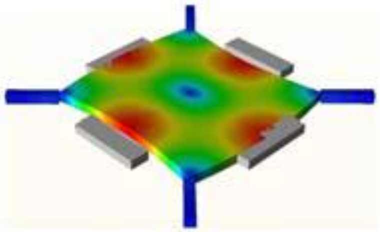
Wineglass Disk (bulk Acoustic mode) Y.-W. Lin et al.(2004)	Poly silicon (3 µm thick)	Disk radius = 32 µm	60 MHz	48,000	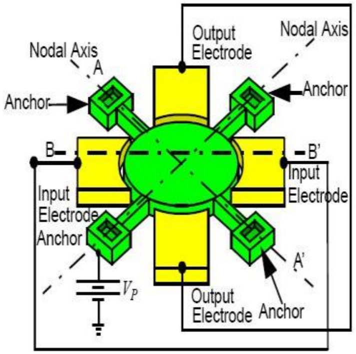
LEE and Seshia(2009)	Single crystal silicon (25 µm thick)	Disk radius = 400 µm	5.43 MHz	1,900,000	

Micromechanical Resonators: Literature Review

Radial contour disk (bulk acoustic) Clark et al.(2005)	Poly silicon (2 µm thick)	Disk radius = 16.7 µm	156 MHz	9,290	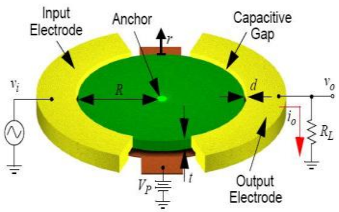
Circular disk (flexural Mode) Huang et al.(2008)	Nickel (3 µm thick)	Disk radius = 15 µm	11.6 MHz	1,651	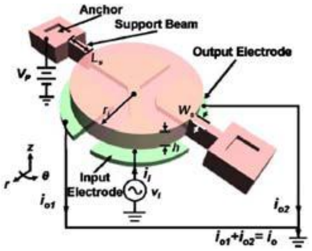
Square plate (flexural mode) Demirici and Nguyen(2006)	Poly silicon (2.2 µm thick)	Side length = 16 µm	68 MHz	15,000	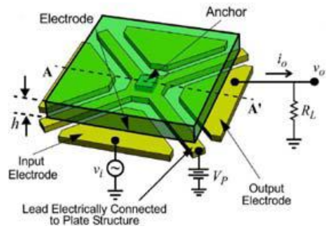
Circular ring (contour mode) S.-S. Li et al.(2004)	Poly silicon (2 µm thick)	Radii: r_i =11.8 µm, and r_o =18.7 µm	1.2 GHz	15,000	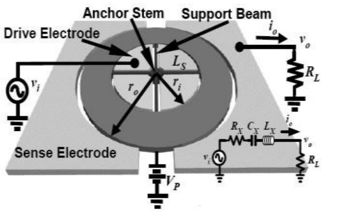

Why Extensional Mode Resonators?

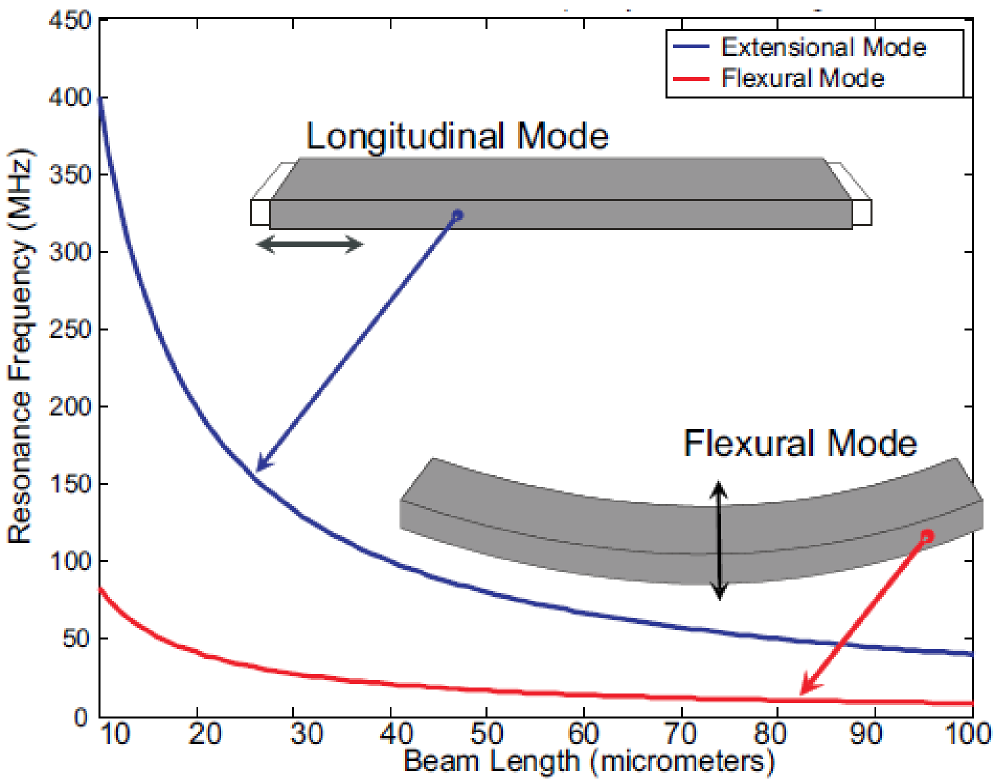

- Extensional mode resonators are much stiffer.
- Much higher frequencies for the same volume of the mechanical structure

Bulk Acoustic Mode of a Disk

(a) Radial-contour (or, breathing) mode where the shape of the disk expands and contracts equally in all the lateral surface.
(b) Elliptical (or, wine-glass) mode where the disk expands along one axis and contracts in the orthogonal axis forming two alternate and perpendicular ellipses per cycle of vibration with four nodal points at the perimeter.

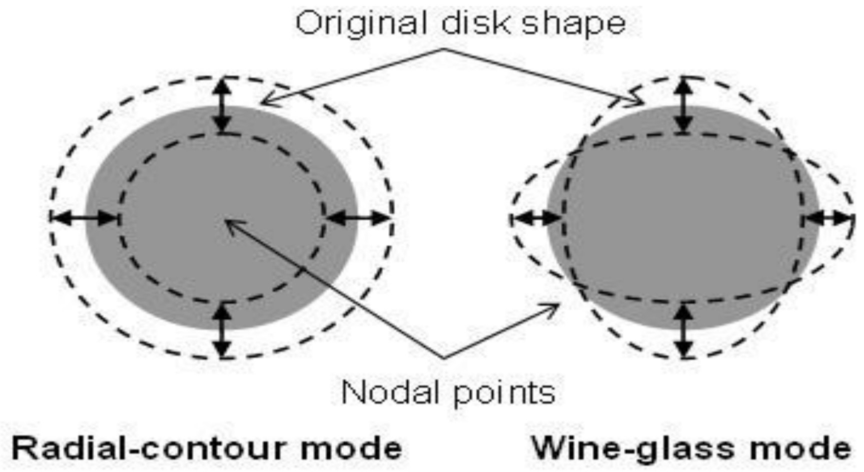

Radial-contour modes provide higher effective stiffness and hence, are preferred.

Popular Structural Material for Micromechanical Resonators

Material	Young's modulus E (GPa)	Density ρ (kg m-3)	Poisson's ratio σ	Deposition temperature (ºC)	Electrical conductivity (107 Ω-1 m-1)
Silicon <110>	165	2,330	0.28	1,000	0.00023
Polysilicon	158	2,300	0.226	588	0.001
Polydiamond	1,144	3,500	0.069	800	0.001
Silicon carbide	415	3,200	0.192	800	0.00083
$PolySi_{0.35}Ge_{0.65}$	146	4,280	0.23	450	0.005
Nickel	180	8,900	0.31	50	1.43

Objectives

1. Design , simulation and characterization of MEMS based radial contour mode disk resonators using surface micromachined poly silicon, electroplated nickel and single crystal silicon (SOI) as structural material for high frequency applications.

2. Design and analysis of alternative extensional mode resonator geometries.

3. Fabrication of the structures using commercial Multi User MEMS Processes (MUMPs®).

4. Performance comparison of the disk resonators realized using different structural material.

5. Performance Comparison of the alternative extensional mode geometries.

6. Realization of MEMS based bandpass filters using laterally clamped and vertically stacked radial-contour mode disk resonators as a proof of concept.

Disk Resonators: Structure

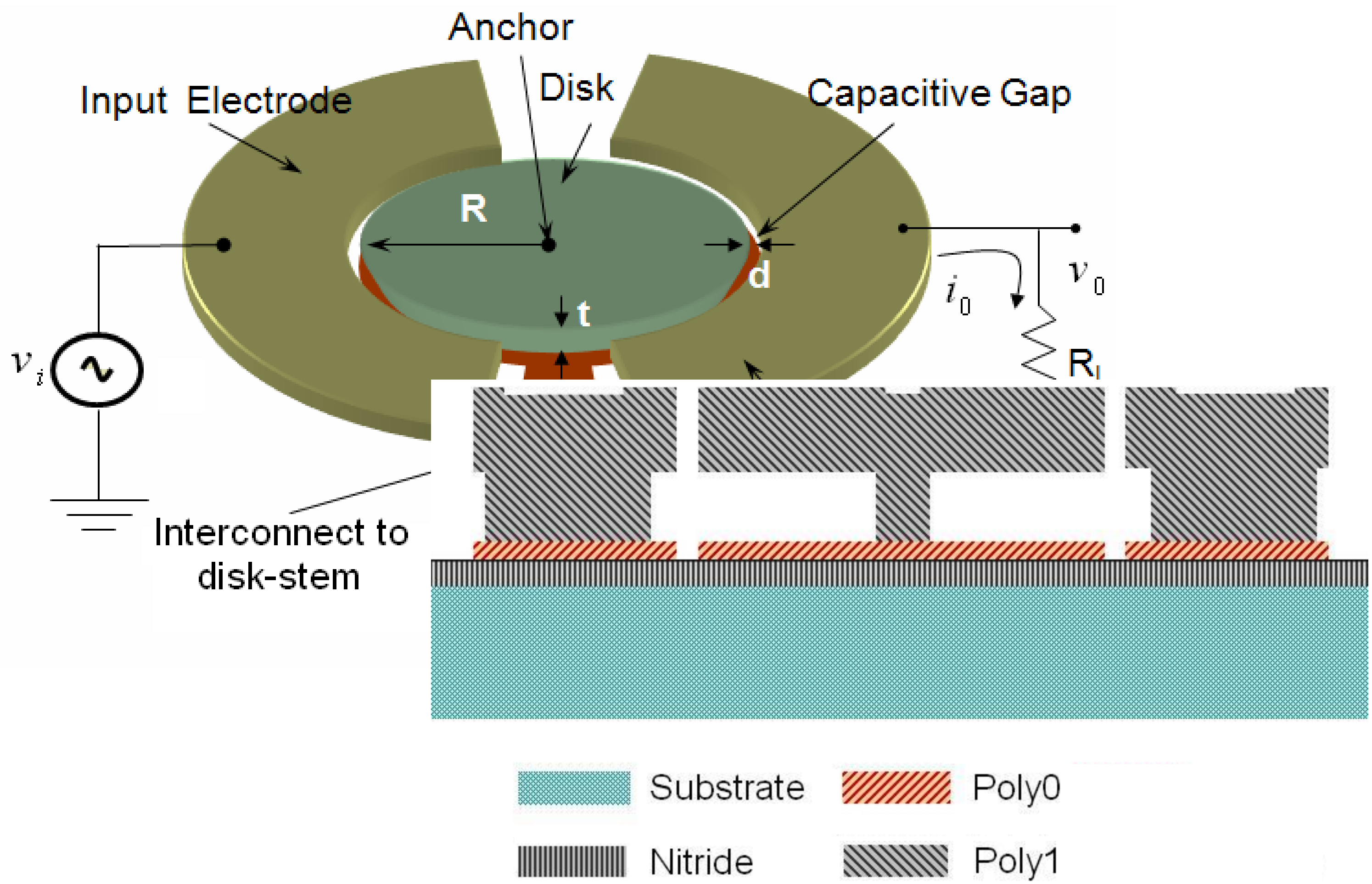

Disk Resonators: Operation

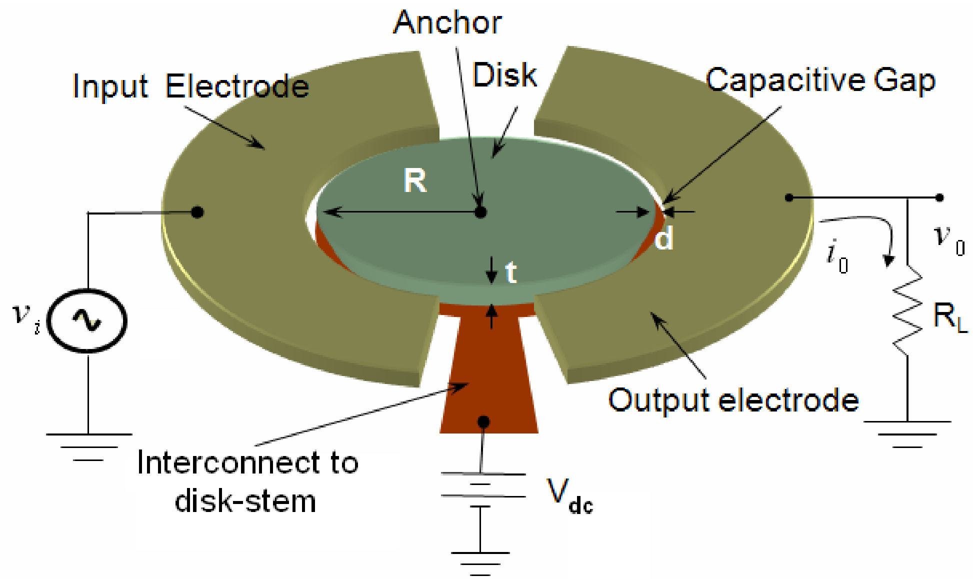

$$f_0 = \frac{\lambda_i}{2\pi R}\sqrt{\frac{E}{\rho(1-\sigma^2)}}$$

$$F_i = V_{dc}\left(\frac{\partial C_1}{\partial r}\right)v_i$$

$$i_0 = V_{dc}\frac{\partial C_2}{\partial t}$$

Same freq. f_0

V_{dc} applied to disk

↓

Sinusoidal v_i applied to disk

↓

Radial electrostatic force F_i on disk

↓

Expansion and contraction of disk

↓

Change in disk to o/p-electrode capacitance

↓

Output motional current i_o

More

Appendix D

- **Disk Resonators: Electrical Model**

$$\begin{bmatrix} i_0 \\ v_i \end{bmatrix} = \begin{bmatrix} 0 & n \\ \frac{1}{n} & 0 \end{bmatrix} \begin{bmatrix} F \\ \dot{r} \end{bmatrix}$$

$$n_k = V_{dc} \frac{\partial C_k}{\partial r} = V_{dc} \frac{\partial}{\partial r} \left(\frac{\varepsilon A_k}{d_0 - r} \right) \approx V_{dc} \left(\frac{\varepsilon A_k}{d_0^2} \right) \quad (\text{for, } r << d)$$

$$L_e = \left(\frac{l_e}{n^2} \right)$$

$$C_e = (n^2 c_e)$$

$$R_e = \left(\frac{r_e}{n^2} \right)$$

$$R_e = \left(\frac{1.18 \text{x} 10^{29}}{Q V_{dc}{}^2} \right) \left(\frac{d^4}{Rt} \right)$$

Back

Appendix C: Mechanical Model

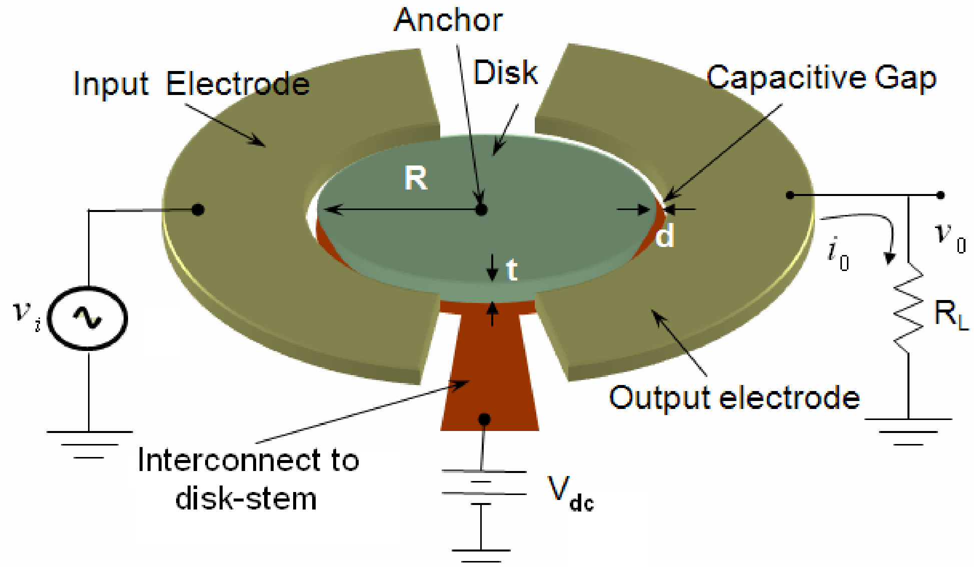

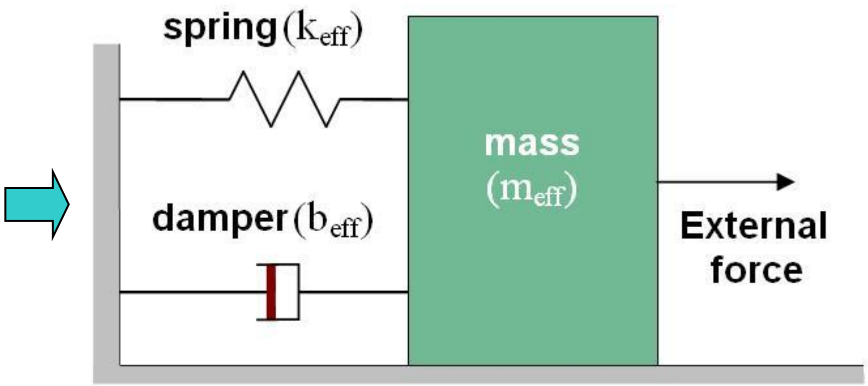

$$m_{eff} = \frac{2E_k}{v^2(R)} = \frac{2\pi\rho t \int_0^R r\, J_1(hr)^2\, dr}{J_1(hR)^2} = \pi\rho t R^2 \left[1 - \frac{J_0(hR) J_2(hR)}{J_1(hR)^2}\right]$$

$$\text{with, } h = \omega_0 \sqrt{\frac{\rho}{\left(\frac{E}{1+\sigma}\right) + \left(\frac{E\sigma}{1-\sigma^2}\right)}} = \frac{\lambda_i}{R}$$

$$\omega_0 = \sqrt{k_{eff} / m_{eff}}$$

$$b_{eff} = \frac{\omega_0 m_{eff}}{Q} = \frac{\sqrt{k_{eff} m_{eff}}}{Q}$$

Disk Resonators: Equivalent Model

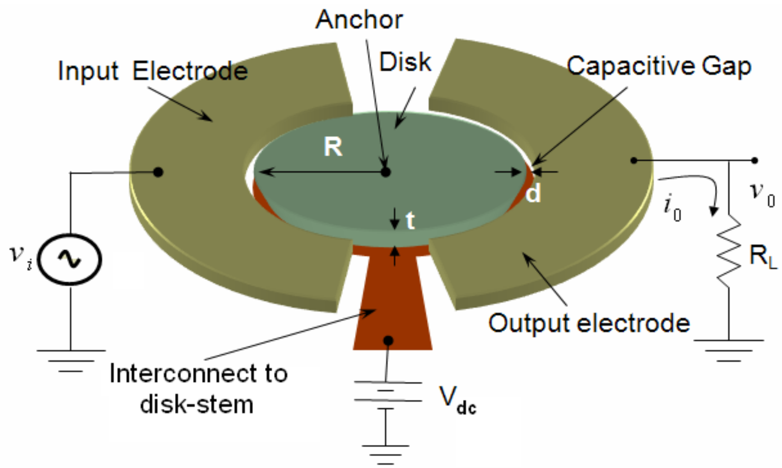

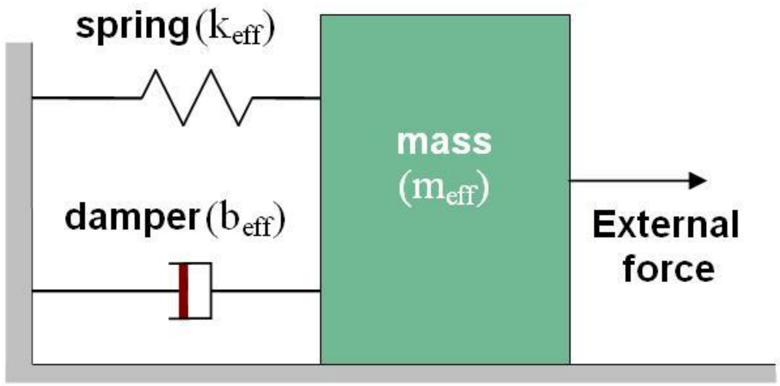

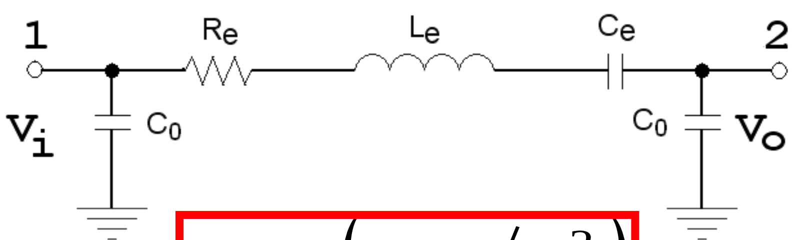

Electrical quantity	Mechanical analog
Voltage (V)	Force (F)
Current (I)	Velocity (v)
Resistance (R)	Damping (b)
Capacitance (C)	Compliance (1/k)
Inductance (L)	Mass (m)

$$L_e = \left(m_{eff} / \eta^2\right)$$

$$R_e = \left(b_{eff} / \eta^2\right)$$

$$C_e = \left(\eta^2 / k_{eff}\right)$$

$$\eta = V_{dc} \frac{\partial C_k}{\partial x}$$

Resonance Frequency Design

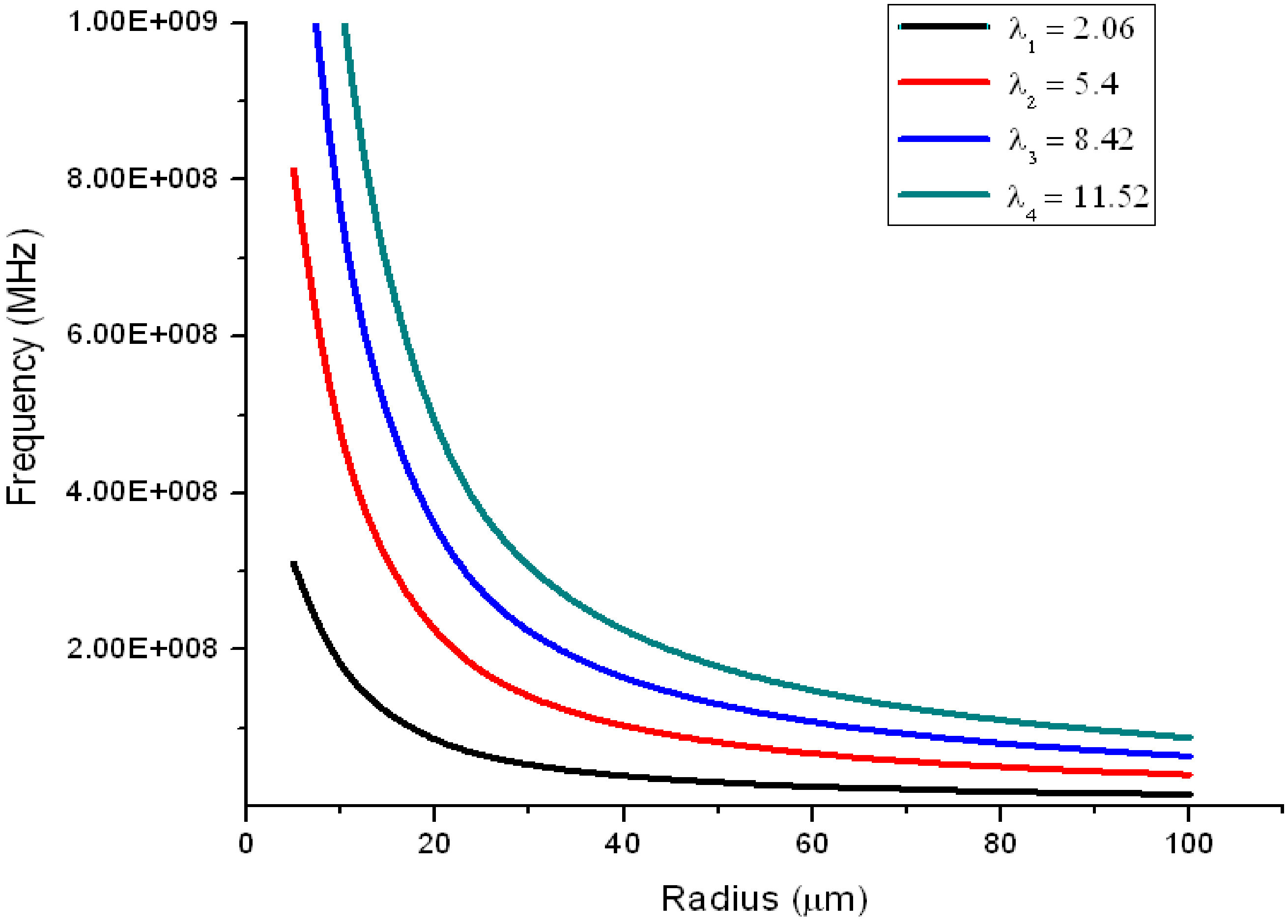

Fig.: Variation of breathing mode resonance frequencies with disk radius using nickel as structural material.

More

Resonance Frequency Design

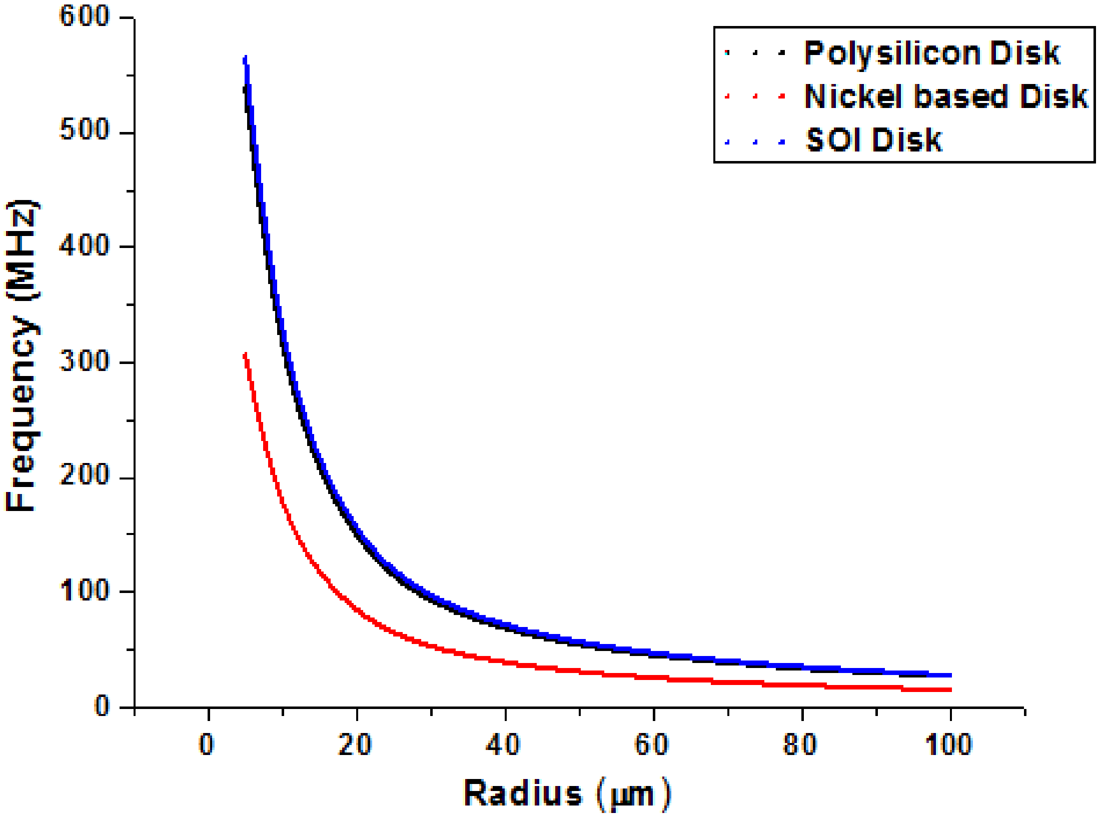

Fig. : Variation of first radial contour mode frequencies with disk radius

Disk Resonators: Equivalent Model

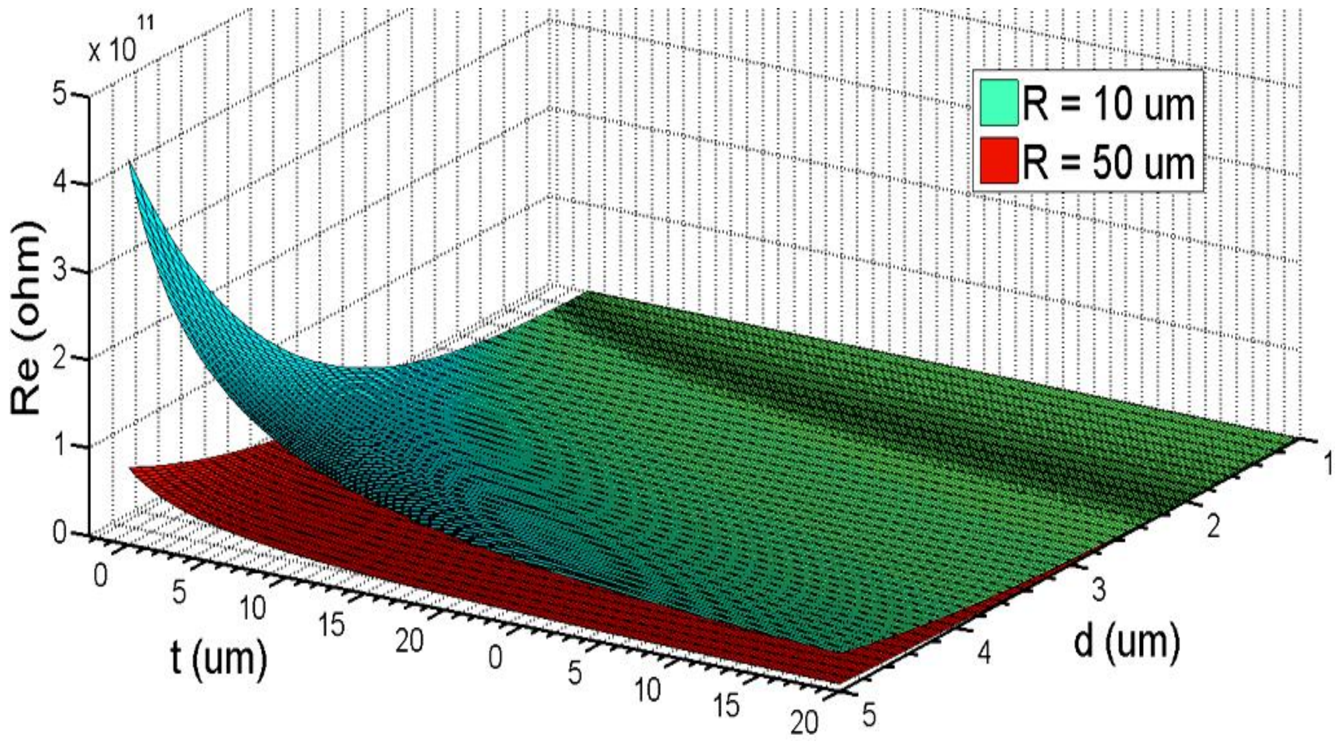

Disk Resonator: Anchored at the Center

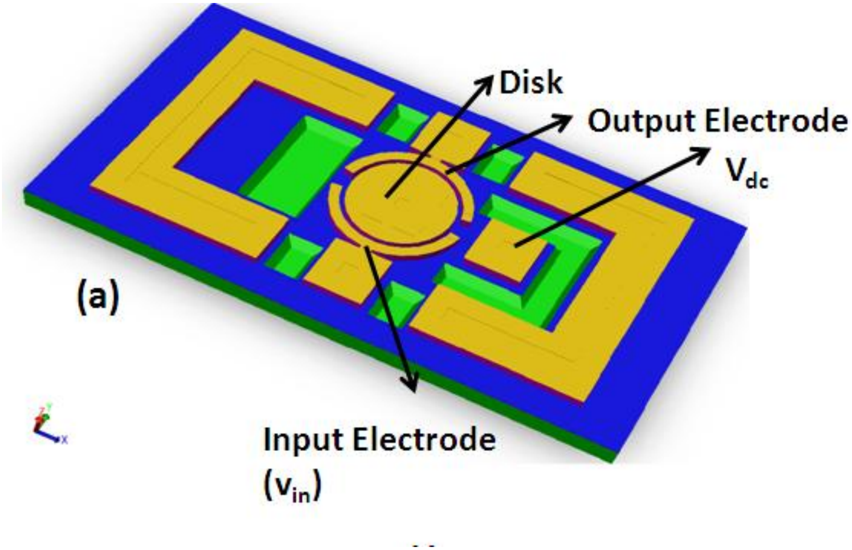

Fig: Bottom Anchored Disk

The Resonant frequency can be calculated as :

$$f_0 = \frac{\lambda_i}{2\pi R}\sqrt{\frac{E}{\rho(1-\sigma^2)}}$$

- The disk is suspended by a narrow cylindrical stem (anchor).
- V_{dc} applied to disk through the anchor

R → Radius of the disk
E → Young's modulus
ρ → mass density
σ → Poisson's ratio

Disk Resonator : Side anchored

This design is compatible with the fabrication processes which has a provision of a trench beneath the structural layer.

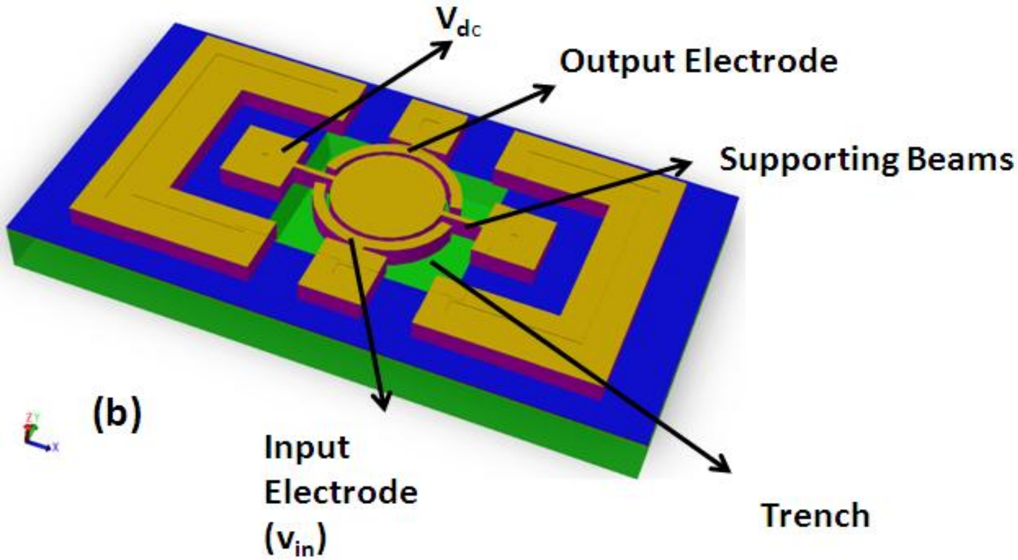

- To minimize the energy loss of the vibration through the anchors, a quarter wavelength long beams should be used. The support-beam length is thus given as:

$$L_s = \frac{1}{4f_0}\sqrt{\frac{E}{\rho}}$$

Disk Resonator Dimensions

Design Parameters	Centrally anchored(Ni)	Centrally anchored(Poly Si)	Side anchored(Ni)	Side anchored(Poly Si)	Side anchored(SOI)
Analytical resonance frequency(MHz)	15.50	27.12	15.50	27.12	27.12
Radius of the disk (µm)	100	99	100	99	104
Thickness of the disk (µm)	20.5*	2*	20.5*	2*	25.5*
Length of the support beam(µm)	___	___	72.5	76	76
Thickness of the support beam (µm)	___	___	20.5*	2*	25*
Disk to electrode gap (µm)	9*	3*	9*	3*	3*

(*indicates values are process limited)

Disk Resonators: Modal Simulation (Ni based)

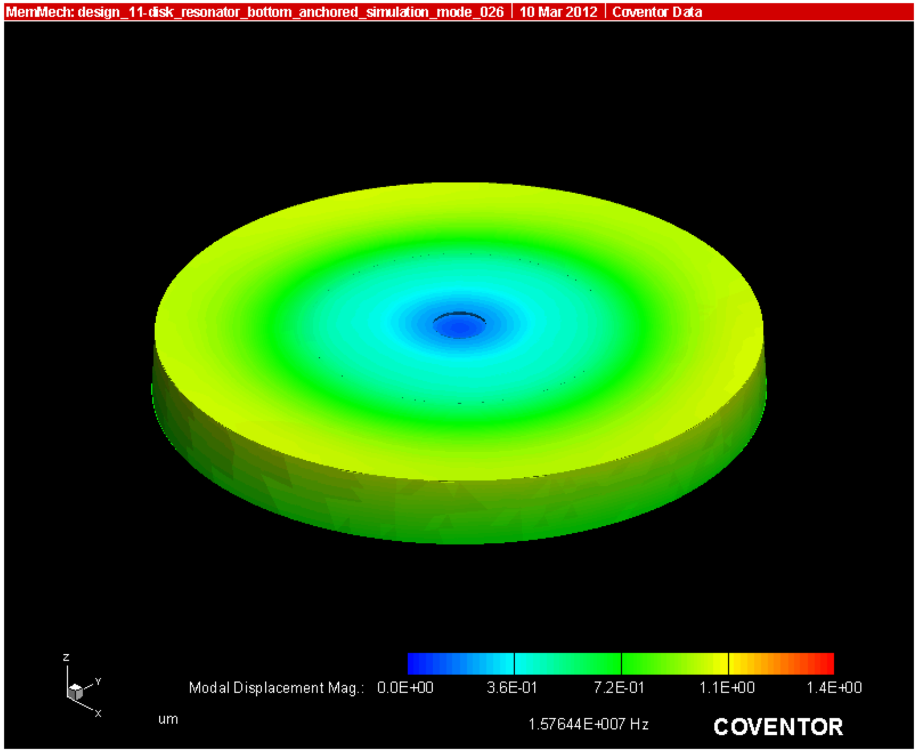

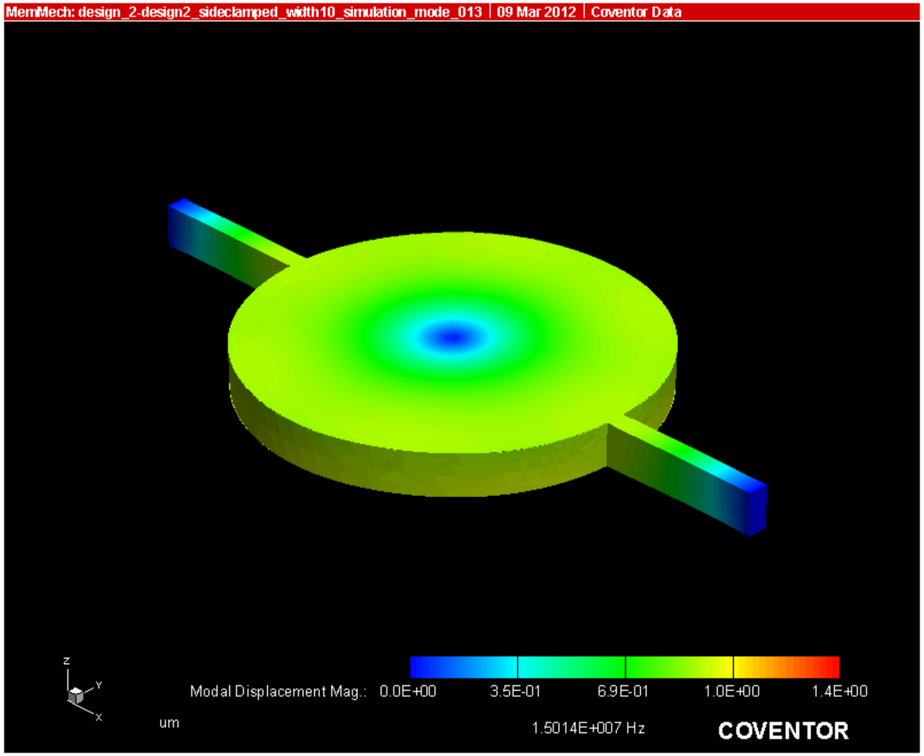

Disk Resonators: Modal Simulation (Poly Si based)

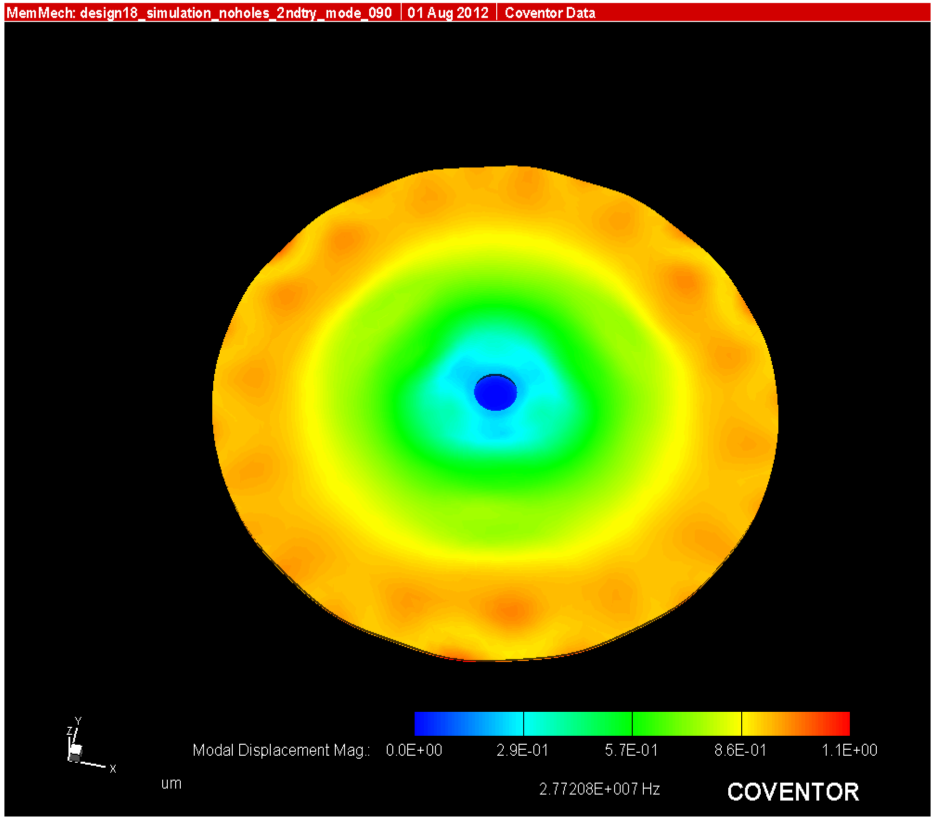

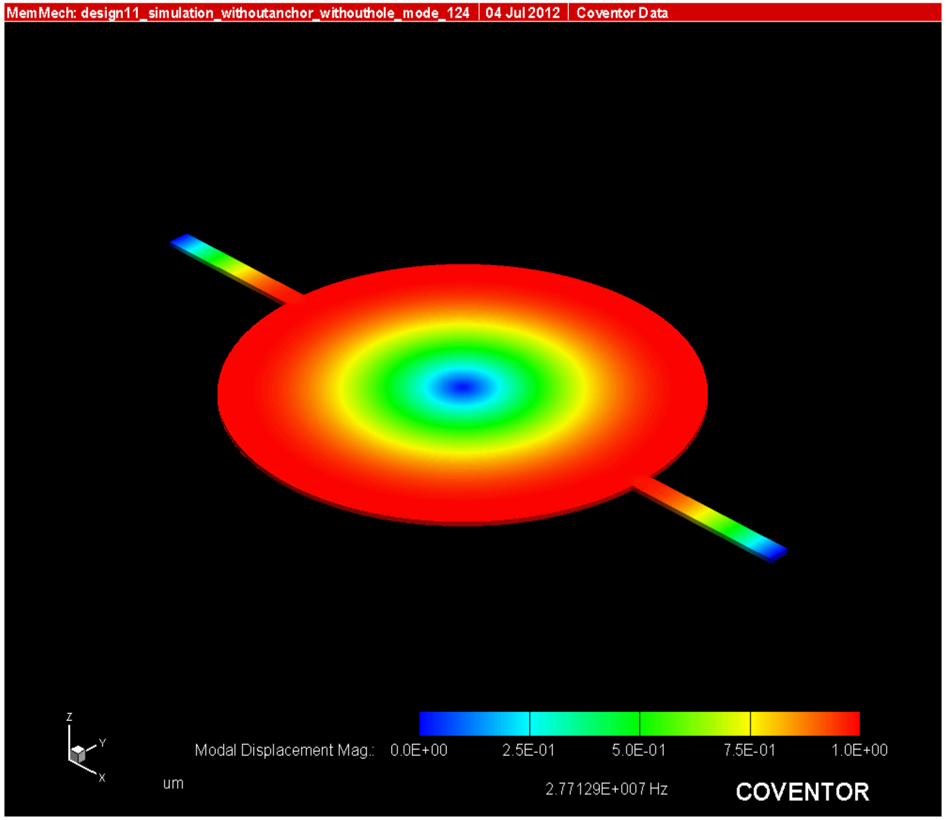

Disk Resonators: Modal Simulation (SOI)

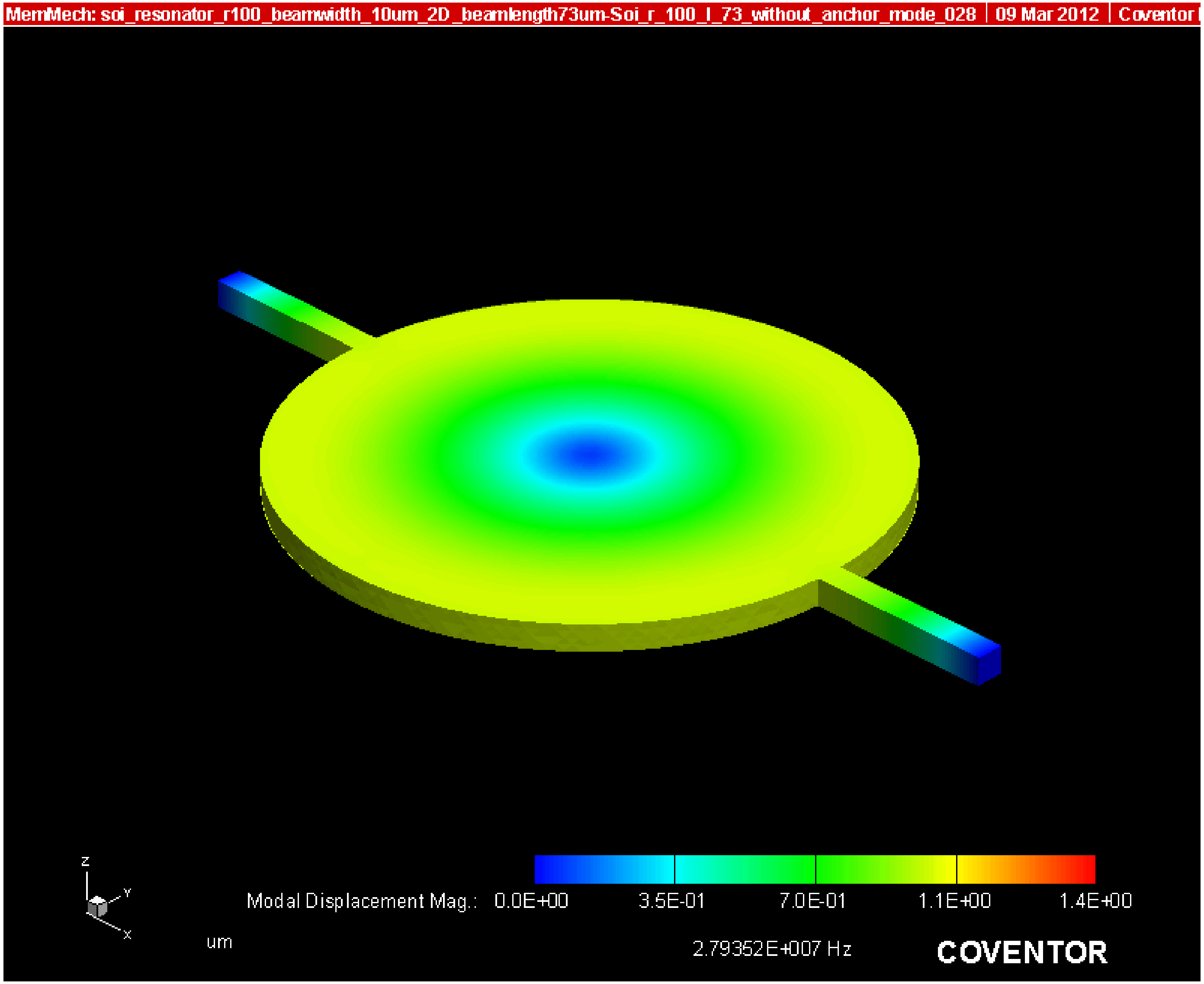

Disk Resonators: Frequency Response

Structural response of the Ni disk resonator subjected to a harmonic excitation:

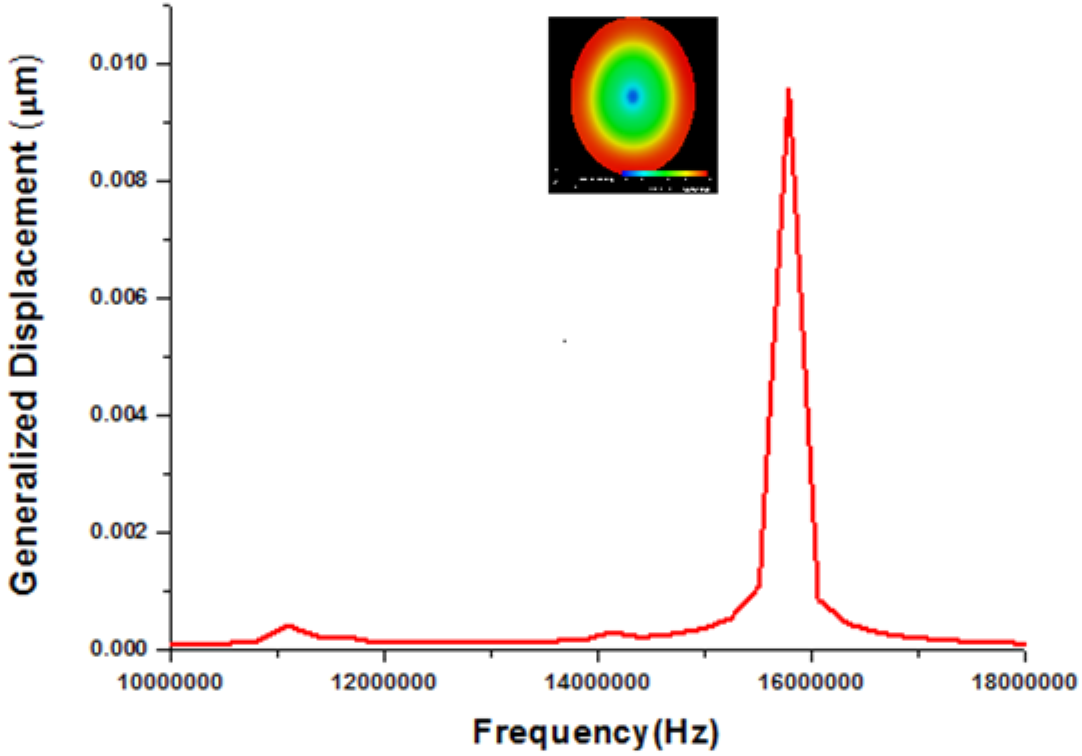

More

Alternative geometries : LBR

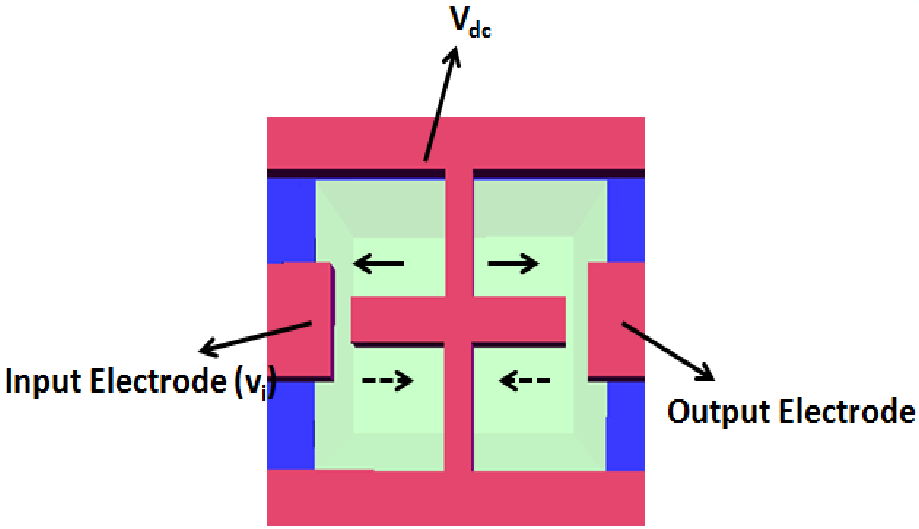

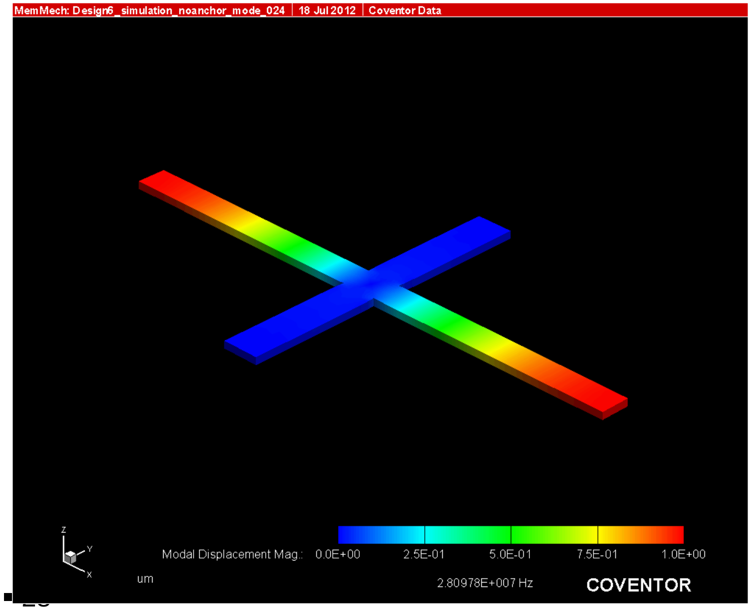

1. This type of structure is therefore the easiest to design and realize for a certain fabrication process.

2. Not a suitable configuration as the transduction area of these beams are very limited.

Alternative geometries : Beam with Flanges

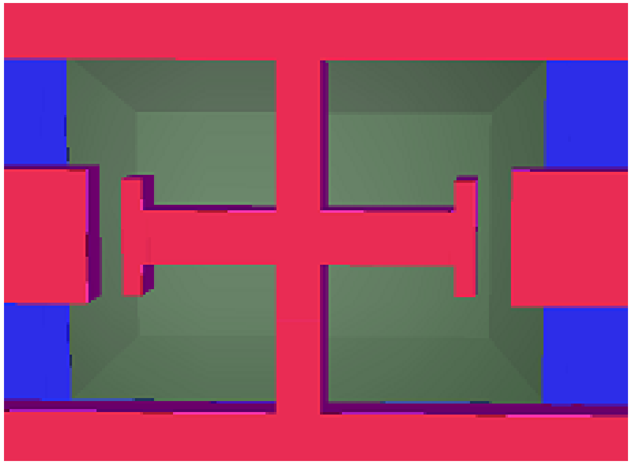

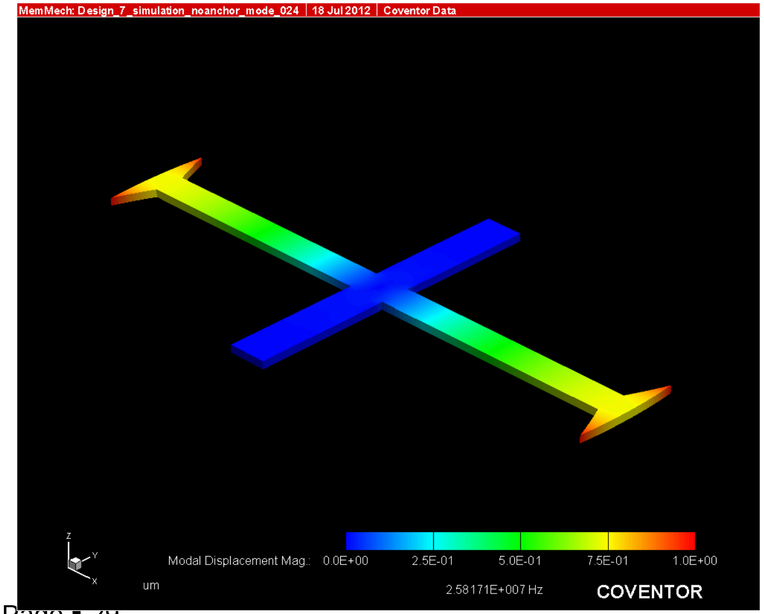

1. For a certain fabrication process where the minimum gap and the thickness of the structural material is predefined, the only way to increase the overlap between the resonator and the electrode .is by increasing the width of the resonator.
2. Difficulty to reach higher frequencies because it is more difficult to design the beam

Alternative geometries : PBR

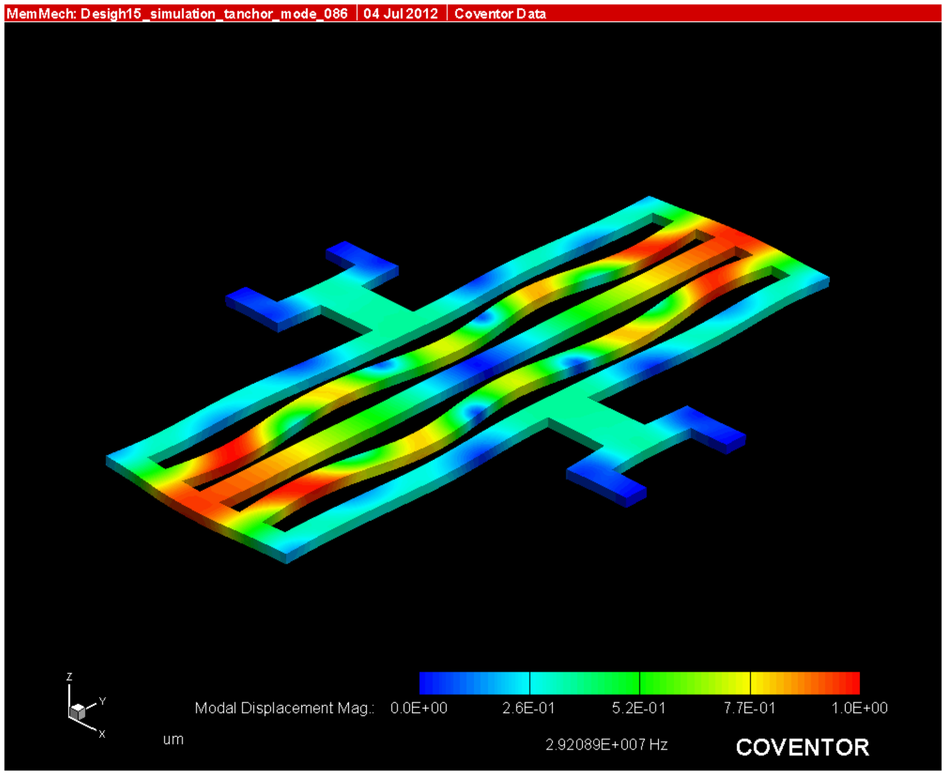

1. This type of MEM resonator is composed of a rectangular membrane fragmented by parallel rectangular holes.
2. Has the unique feature that the resonance frequency is governed by the geometry of a single beam (mainly, its length) while the transduction area is related to the number of connected beams or the.

This design is the best option for realizing longitudinal beam based resonators for high frequency applications.

Alternative geometries : Square Plate

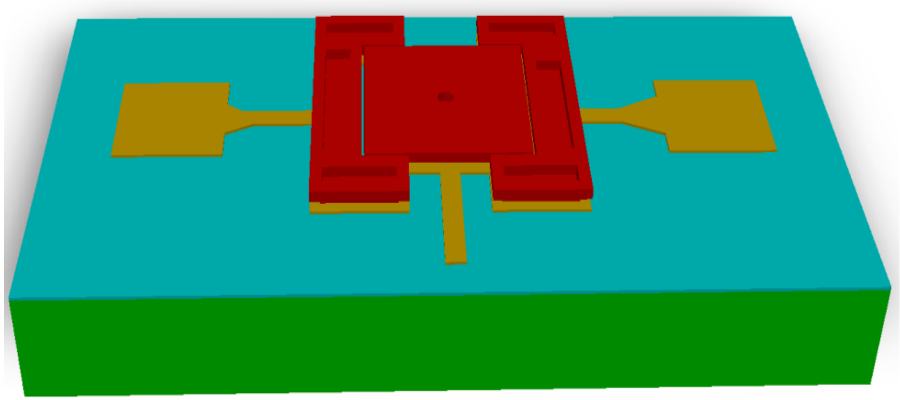

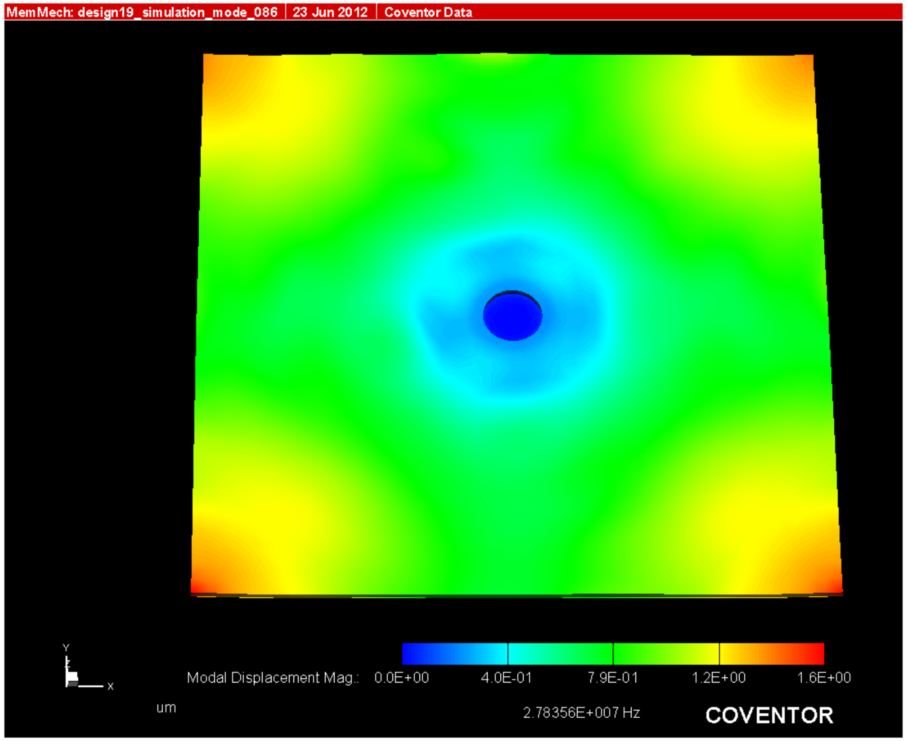

1. Easier to integrate in a process as the design only has straight edges.
2. Air-gap can be reduced a bit here in comparison to that for a circular-disk resonator fabricated using the same process.
3. The main disadvantage of these resonators is that the maximum transduction occur at the four corners than the sides of the plate.

Alternative geometries : Hexagonal Plate

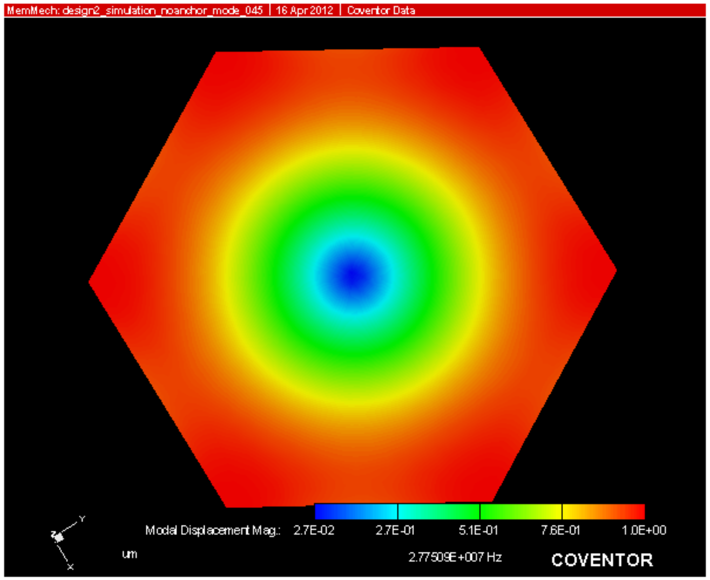

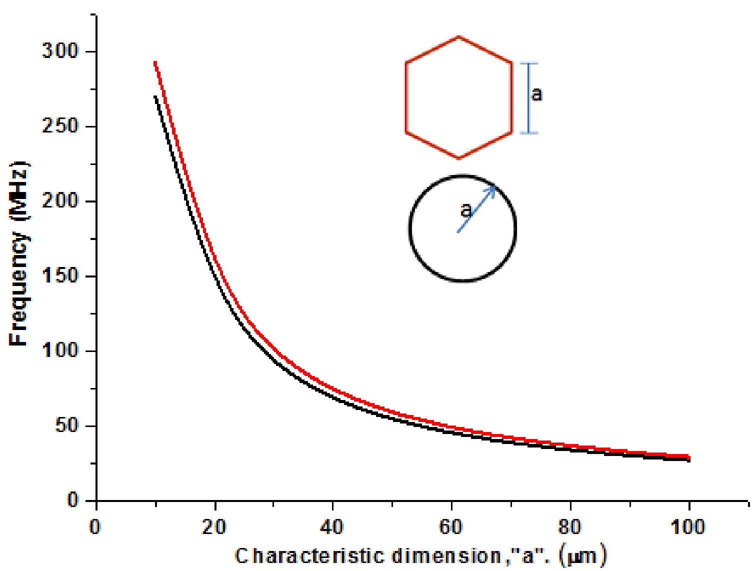

1. The extensional mode vibration pattern of the hexagonal geometry is very similar in nature with the disk structure.

2. The transduction gap between the resonator and electrodes can be reduced for the hexagonal structure following the design rules since it has straight edges; and therefore, shows enhanced performance

Very attractive and practical alternative to the widely demonstrated micromechanical disk resonators, as they provide enhanced performance for a given specification.

Fabrication Using PolyMUMPs

- *PolyMUMPs* process file from *CoventorWare* foundry processes library

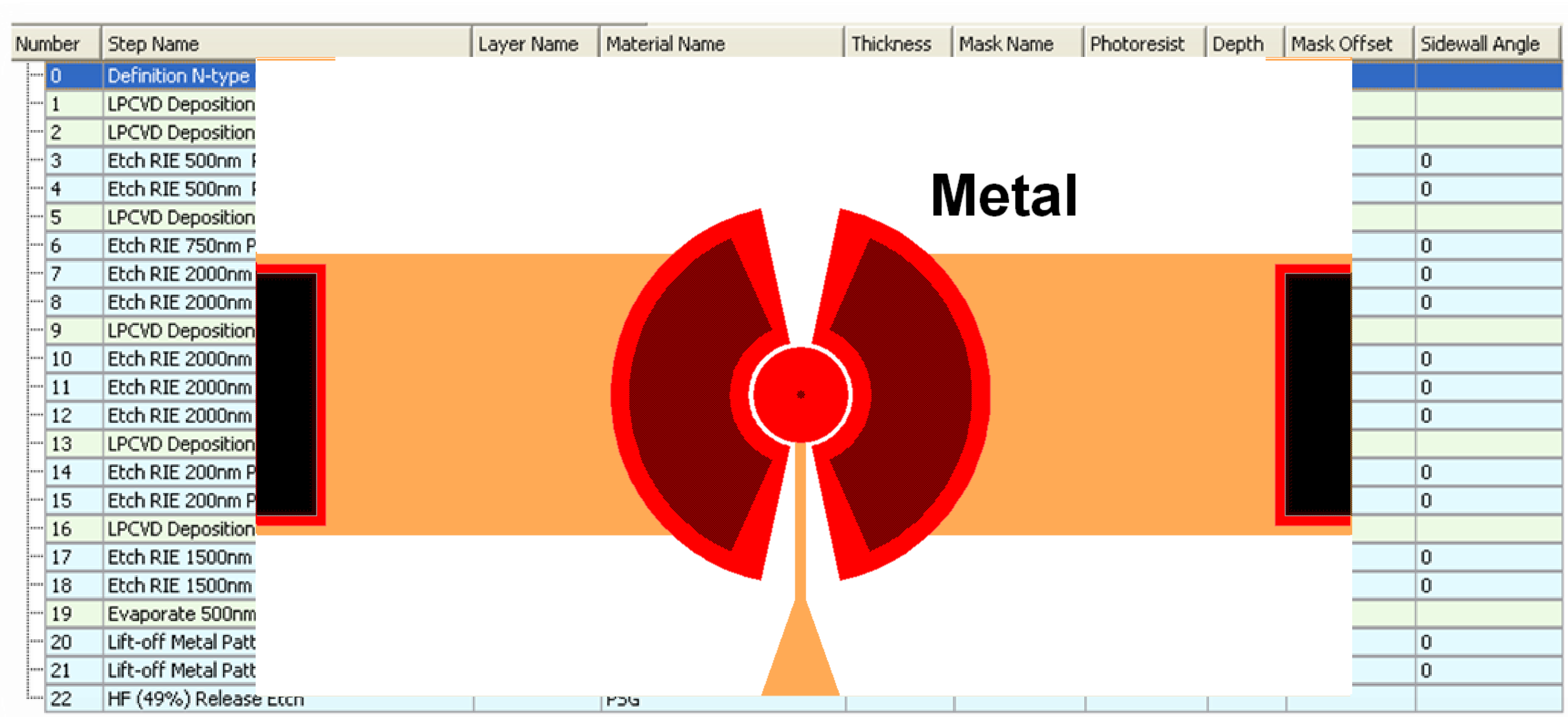

T K Bhattacharyya, E&ECE, IIT Kharagpur

Micrographs of Fabricated Devices

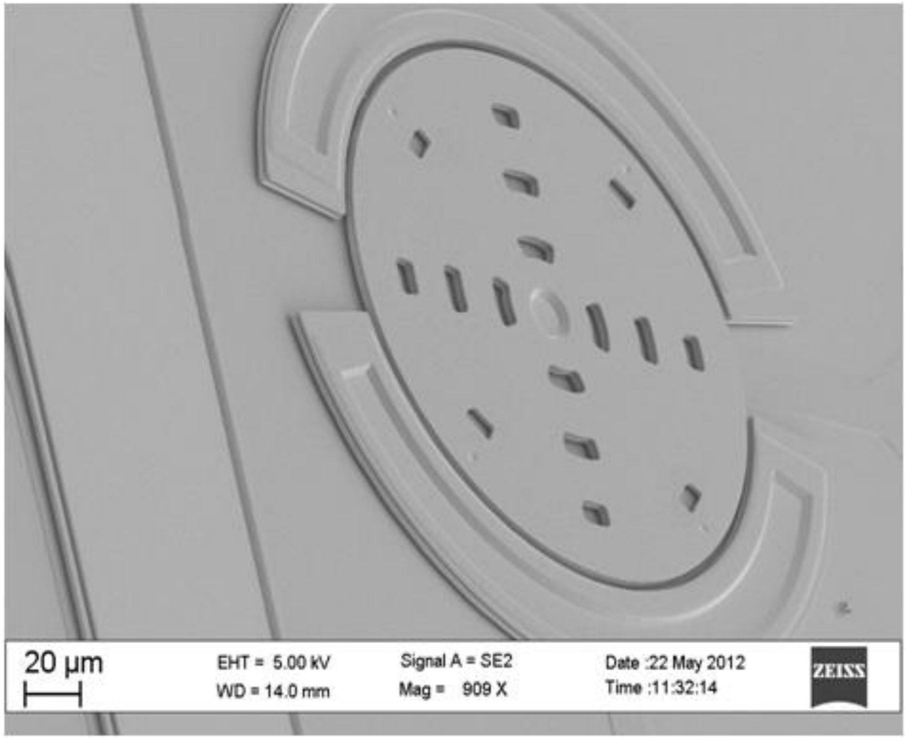

Bottom Anchored Disk

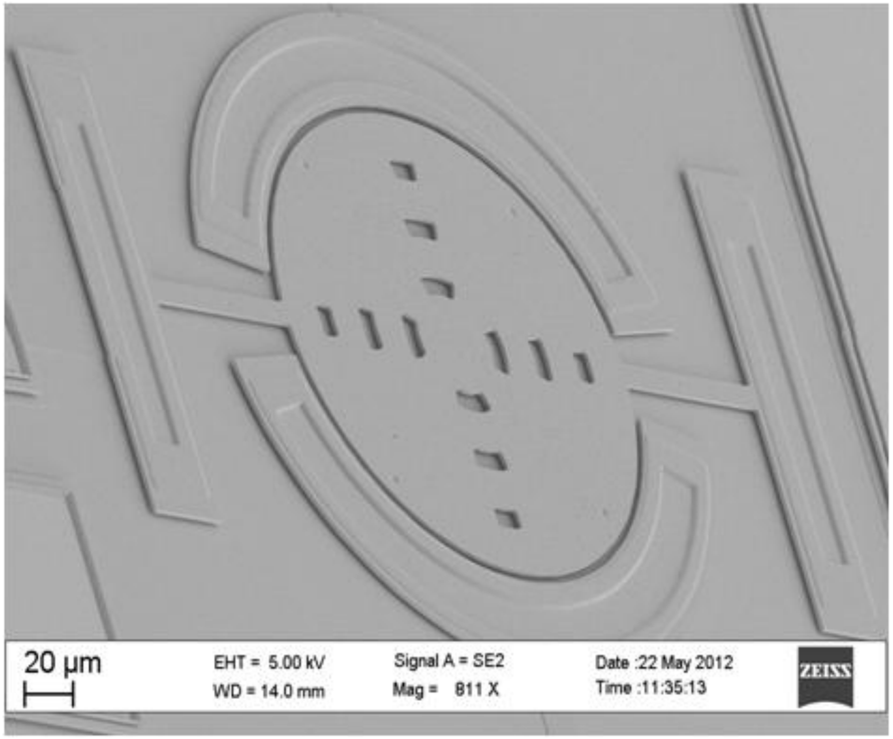

Disk Supported at Periphery

Micrographs of Fabricated Devices (Alternative Geometries)

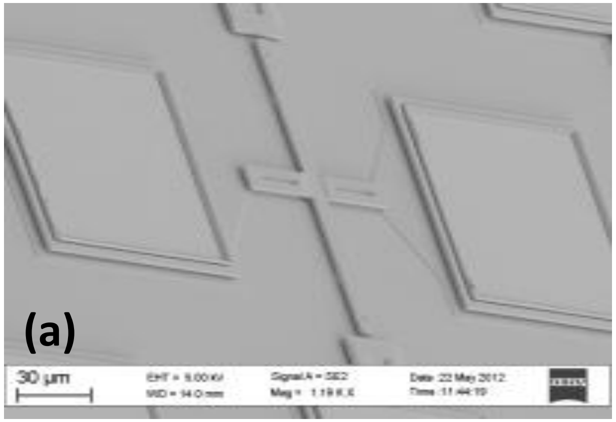

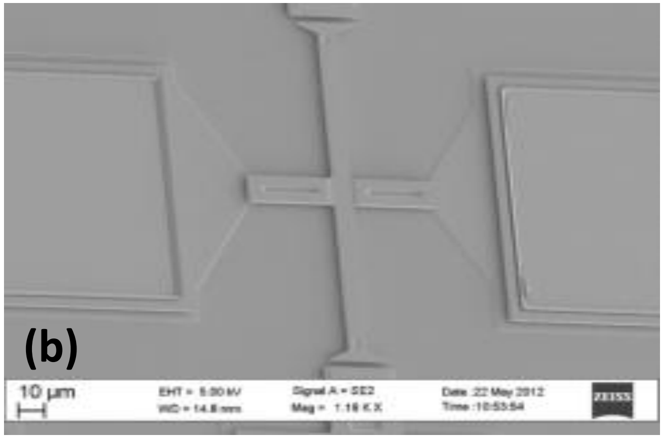

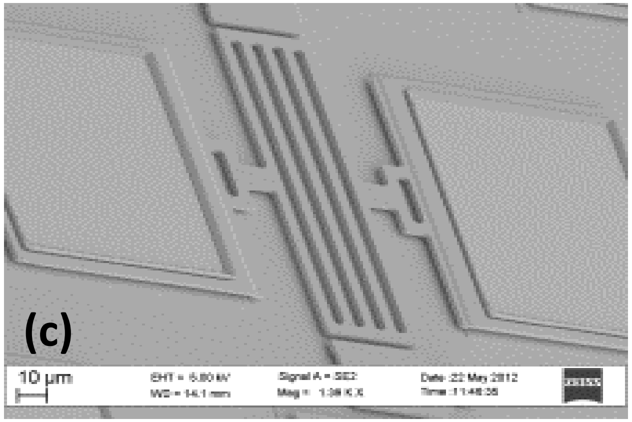

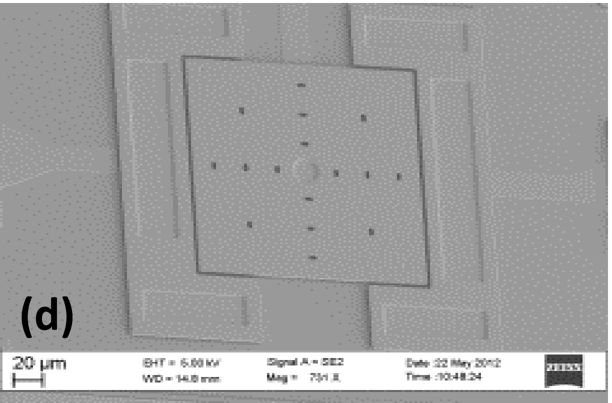

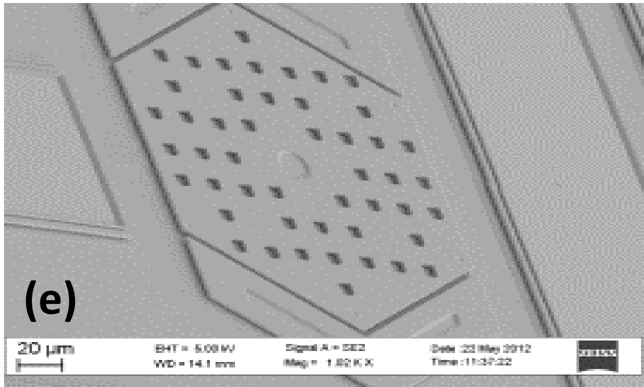

MetalMUMPs Micromachining Process

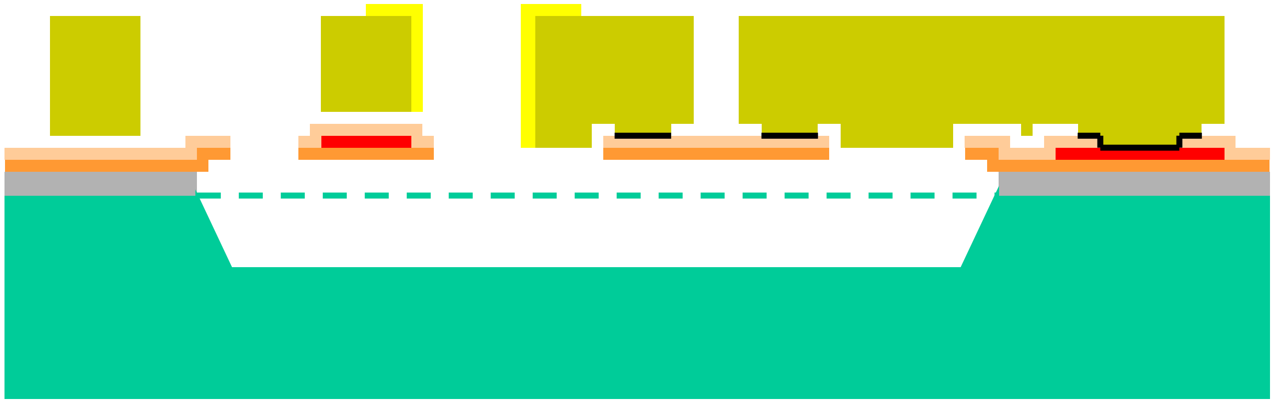

(1) Electroplated nickel is used as the primary structural material and electrical interconnect layer

(2) Doped polysilicon can be used for resistors, additional mechanical structures, and/or cross-over electrical routing.

(3) Silicon nitride is used as an electrical isolation layer

(4) Deposited oxide is used for the sacrificial layers

(5) A trench layer in the silicon substrate can be incorporated for additional thermal and electrical isolation

Substrate	Oxide 1	Poly	Oxide 2	Metal
Isolation Oxide	Nitride 1	Nitride 2	Anchor Metal	Sidewall Metal
Photoresist				

Micrographs of Fabricated Devices

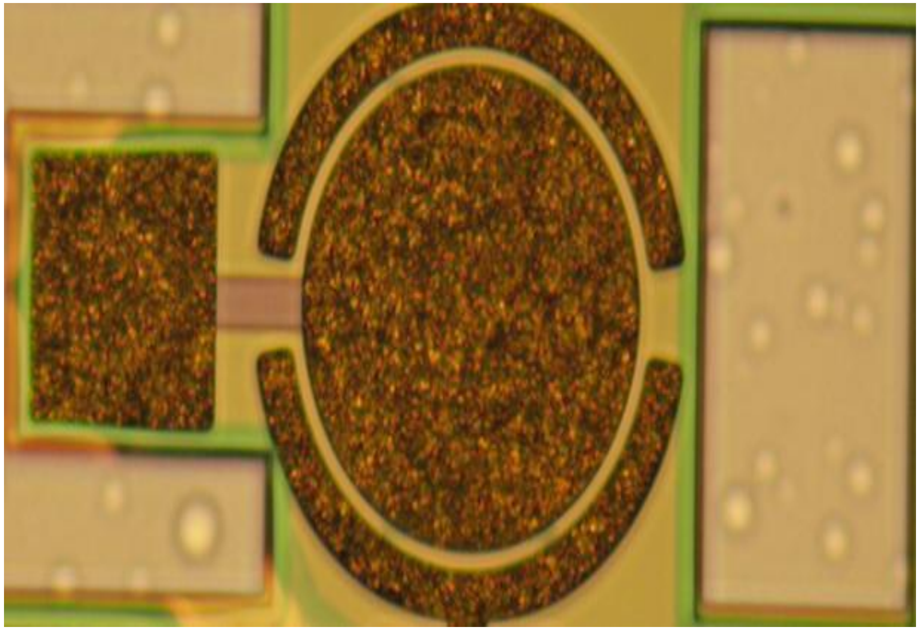

Bottom Anchored Disk

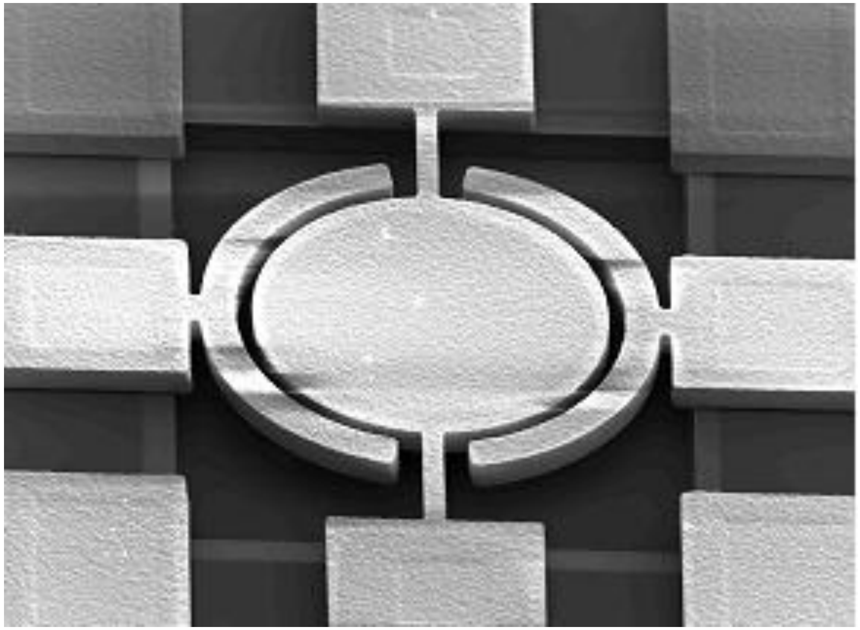

Disk Supported at Periphery

SOI Micromachining Process

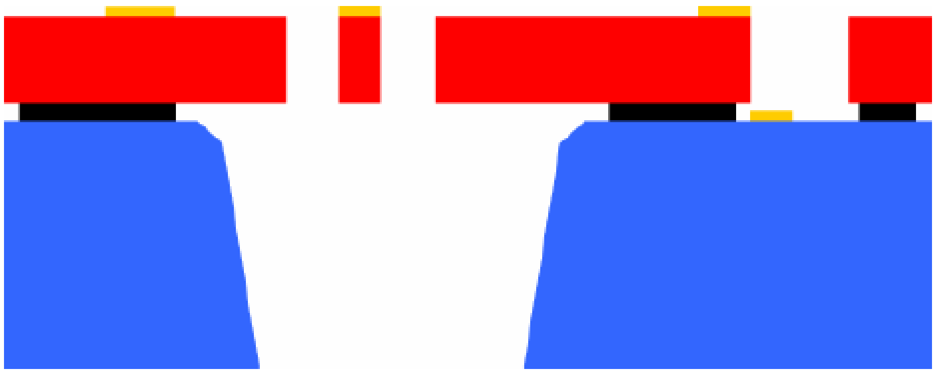

Silicon	Substrate	Bottom Oxide	Shadow Mask
Oxide	Metal	PSG (dopant)	Frontside Protection Material

(1) A silicon-on-insulator (SOI) wafer is used as the starting substrate:
- **Silicon thickness:10 ± 1 mm or 25 ± 1 µm**
- **Oxide thickness:1 ± 0.05 mm (10 mm) or 2 ± 0.05 mm (25 mm)**
- **Handle wafer (Substrate) thickness:400 ± 5 mm**

(2) The Silicon layer is patterned and etched down to the Oxide layer. This layer can be used for mechanical structures, resistor structures, and/or electrical routing.

(3) The Substrate can be patterned and etched from the “bottom” side to the Oxide layer. This allows for through-hole structures.

(4) A shadow-masked metal process is used to provide coarse Metal features such as bond pads, electrical routing, and optical mirror surfaces.

T K Bhattacharyya, E&ECE, IIT Kharagpur

SOI Disk Resonators: 3D Structure

- V_{dc} applied to disk through the Anchors

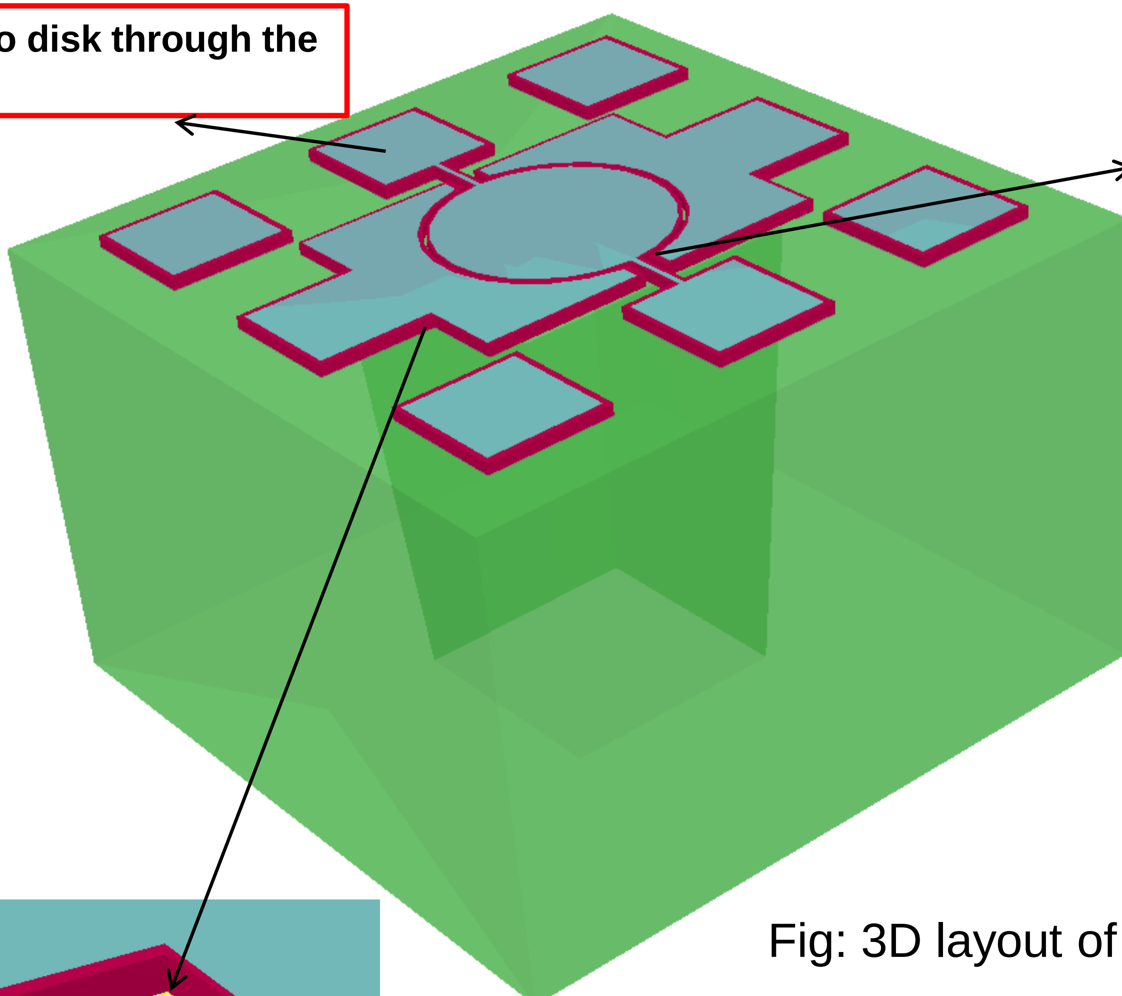

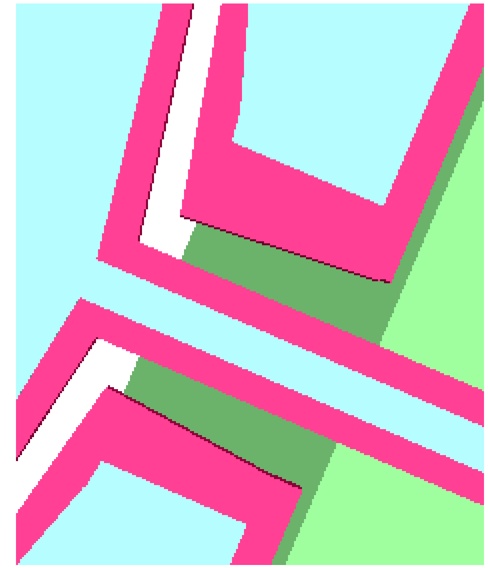

Air gap between electrode and disk, $d_0 \rightarrow 3\ \mu m$

Fig: 3D layout of the disk resonator

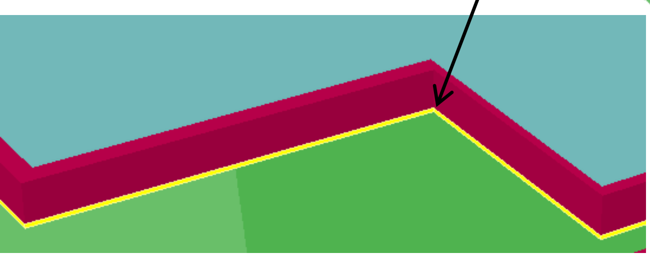

1 μm thick Oxide layer underneath the SOI layer

Micrographs of Fabricated Device

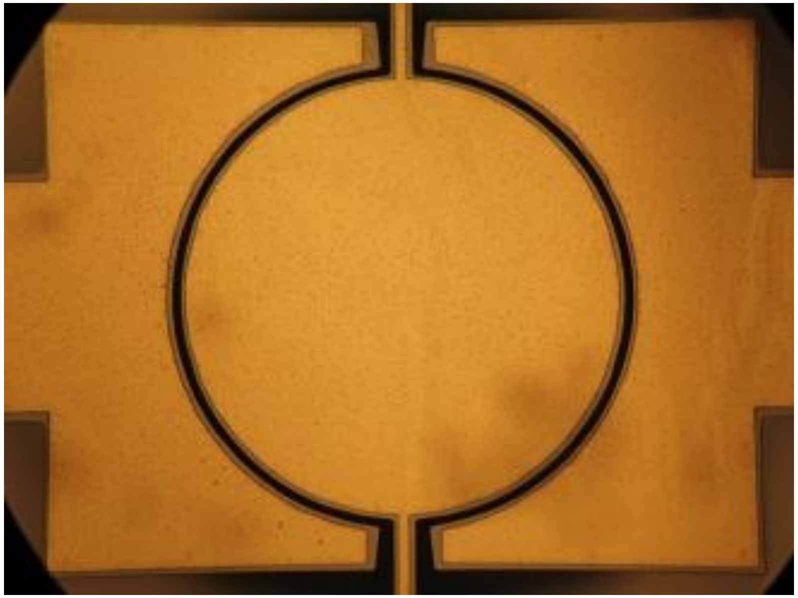

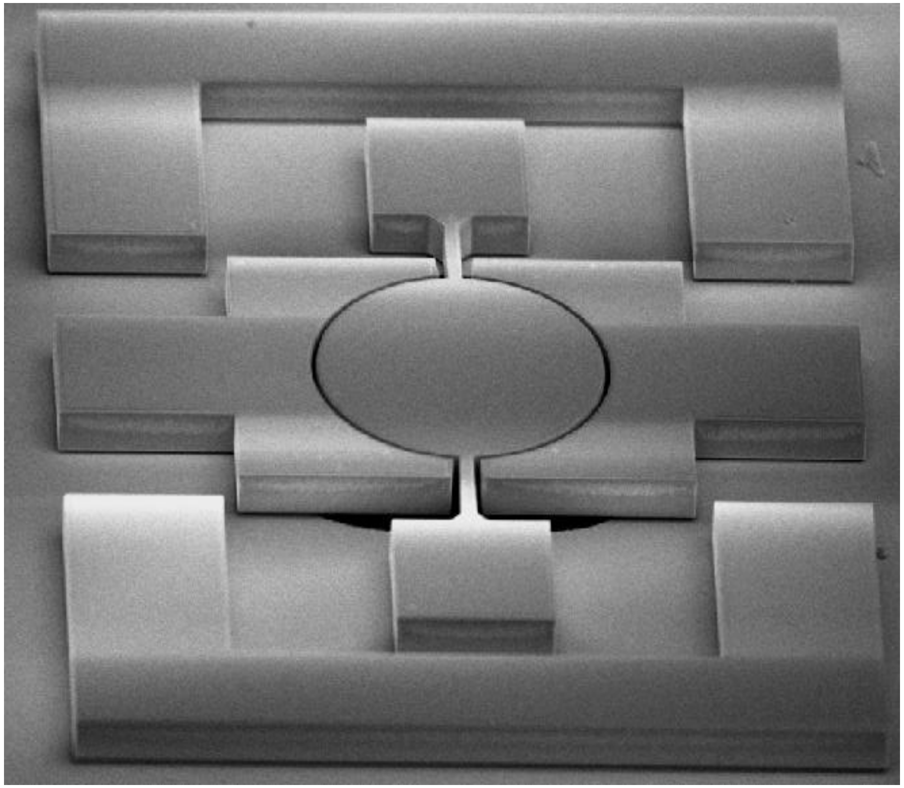

Characterization : Material

From the EDS spectrum, it can be clearly seen that the structural layer of the MetalMUMPs® resonators consist of both gold and nickel and for PolyMUMPs® resonators the structural layer consists of only silicon.

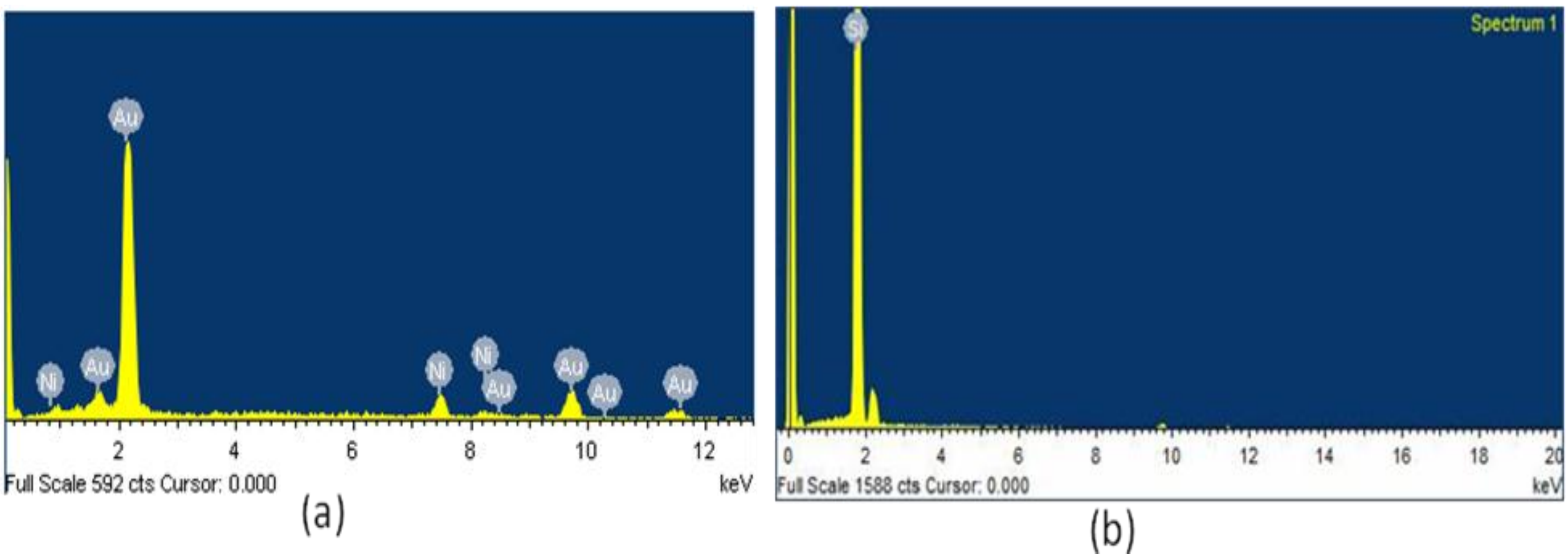

Fig. : EDS spectrum of the structural layer of the MetalMUMPs® (a) and PolyMUMPs® (b) resonators

Characterization : Surface Roughness Measurements

The measured roughness are 145 nm for the gold layer (nickel based process) and 12.4 nm for the polysilicon layer(polysilicon based process) and 2.01 nm for the SOI layer.

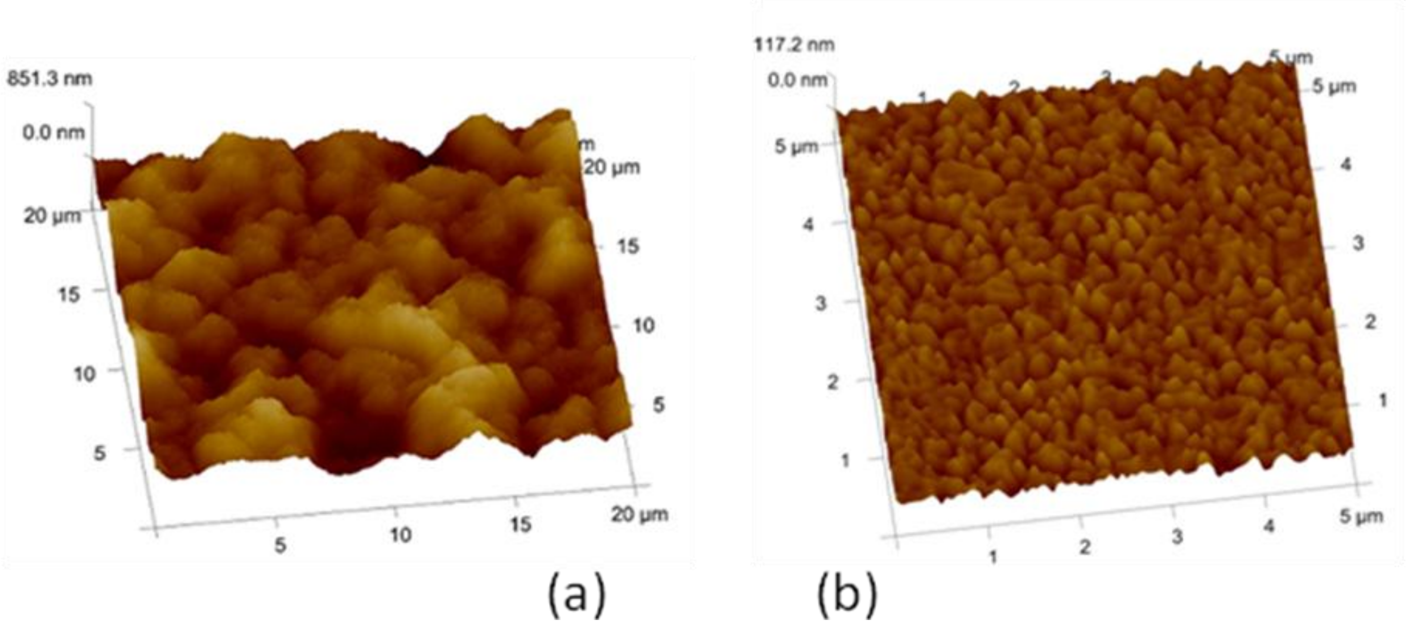

Fig: 3D AFM image of the surface of the gold layer of MetalMUMPs (a) and surface of the POLY1 layer of PolyMUMPs (b).

Characterization :3D Topography

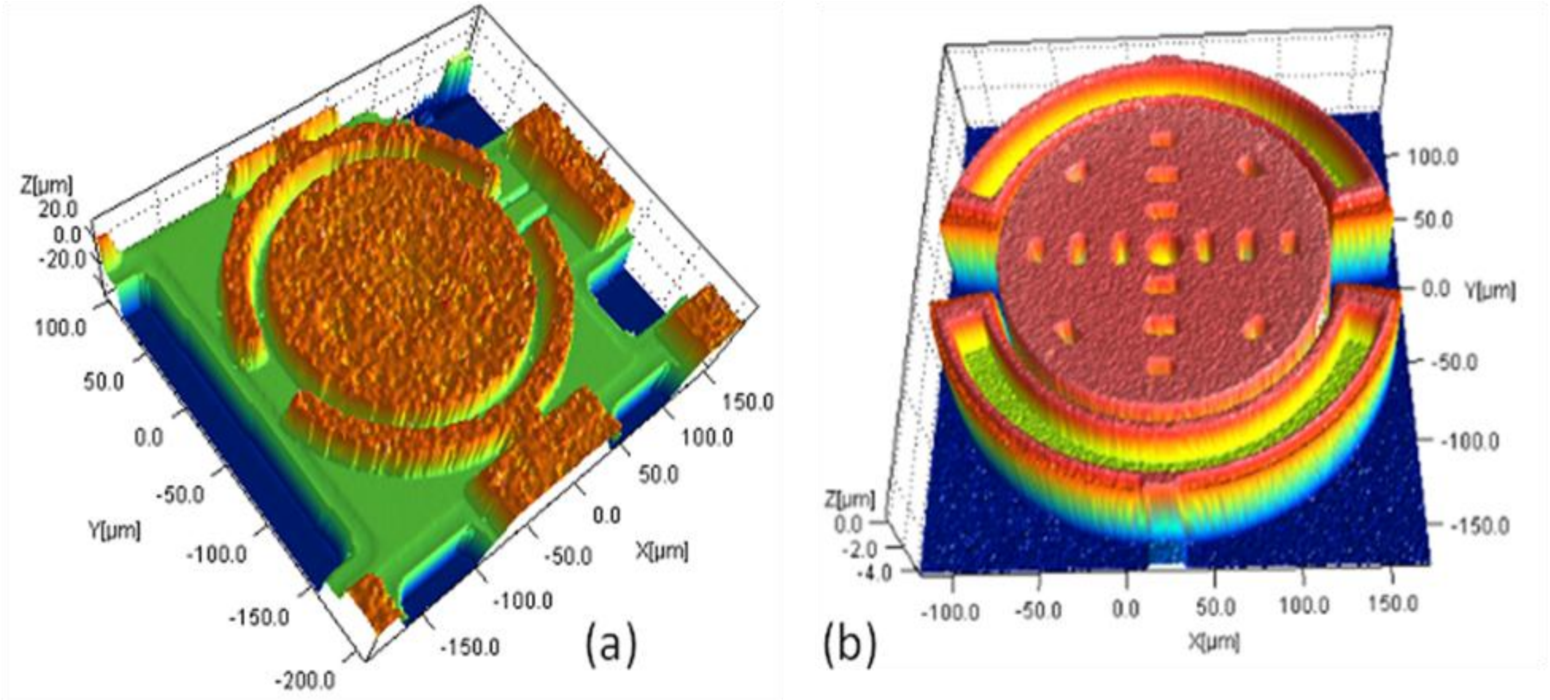

Fig. : 3D view of the measured topography of the nickel based (a) and polysilicon based (b) disk.

Characterization :3D Topography

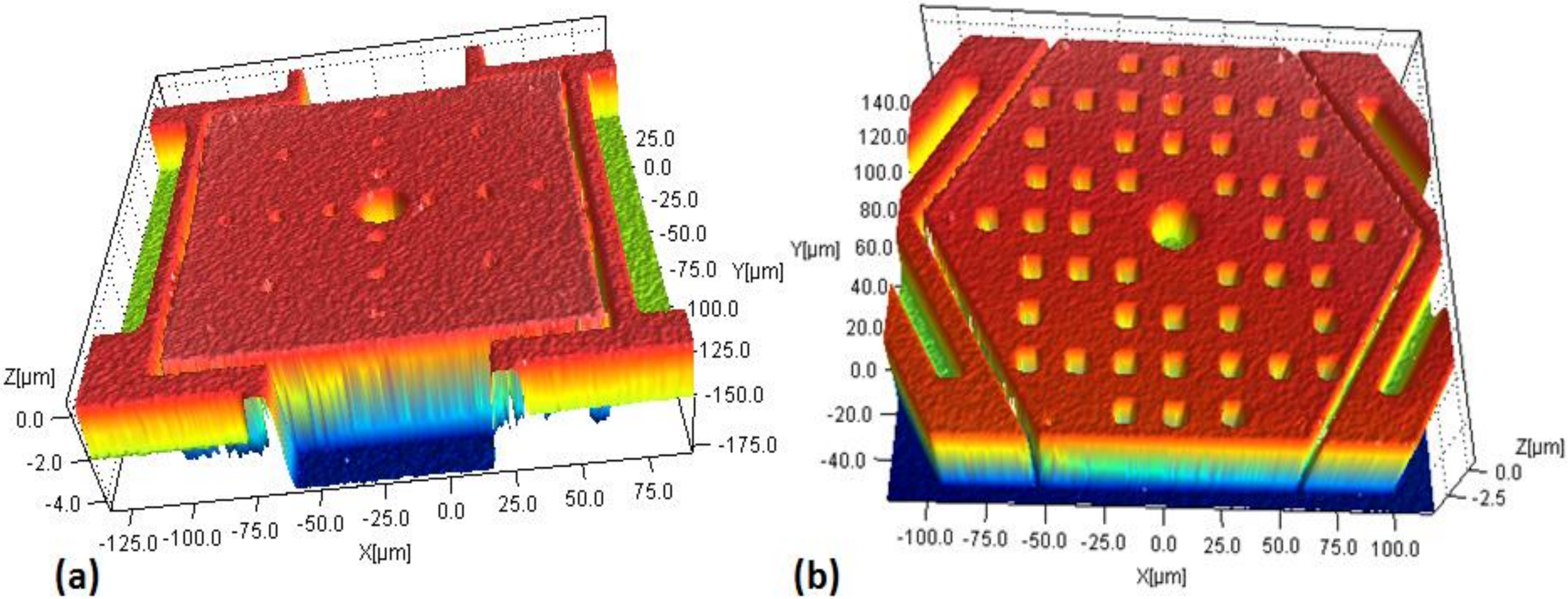

Fig. : 3D view of the measured topography of the square (a) and hexagonal (b) geometry

Mechanical Characterization

- **Laser Doppler Vibrometry (LDV) of a disk resonator:**

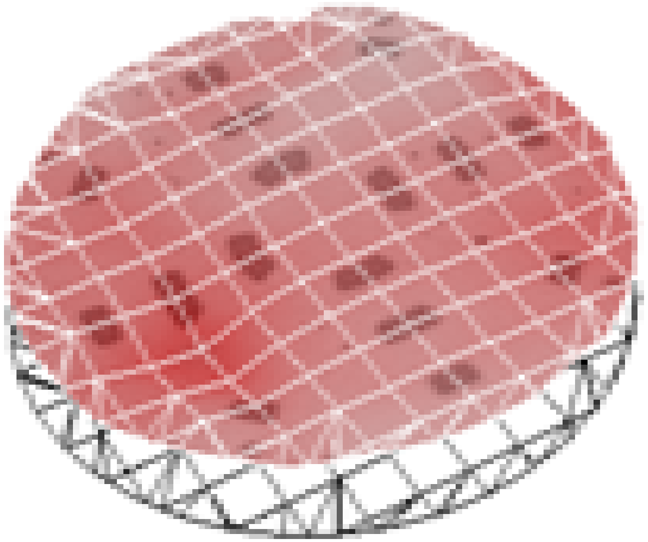

This confirms the proper release of the structure

Mechanical Characterization

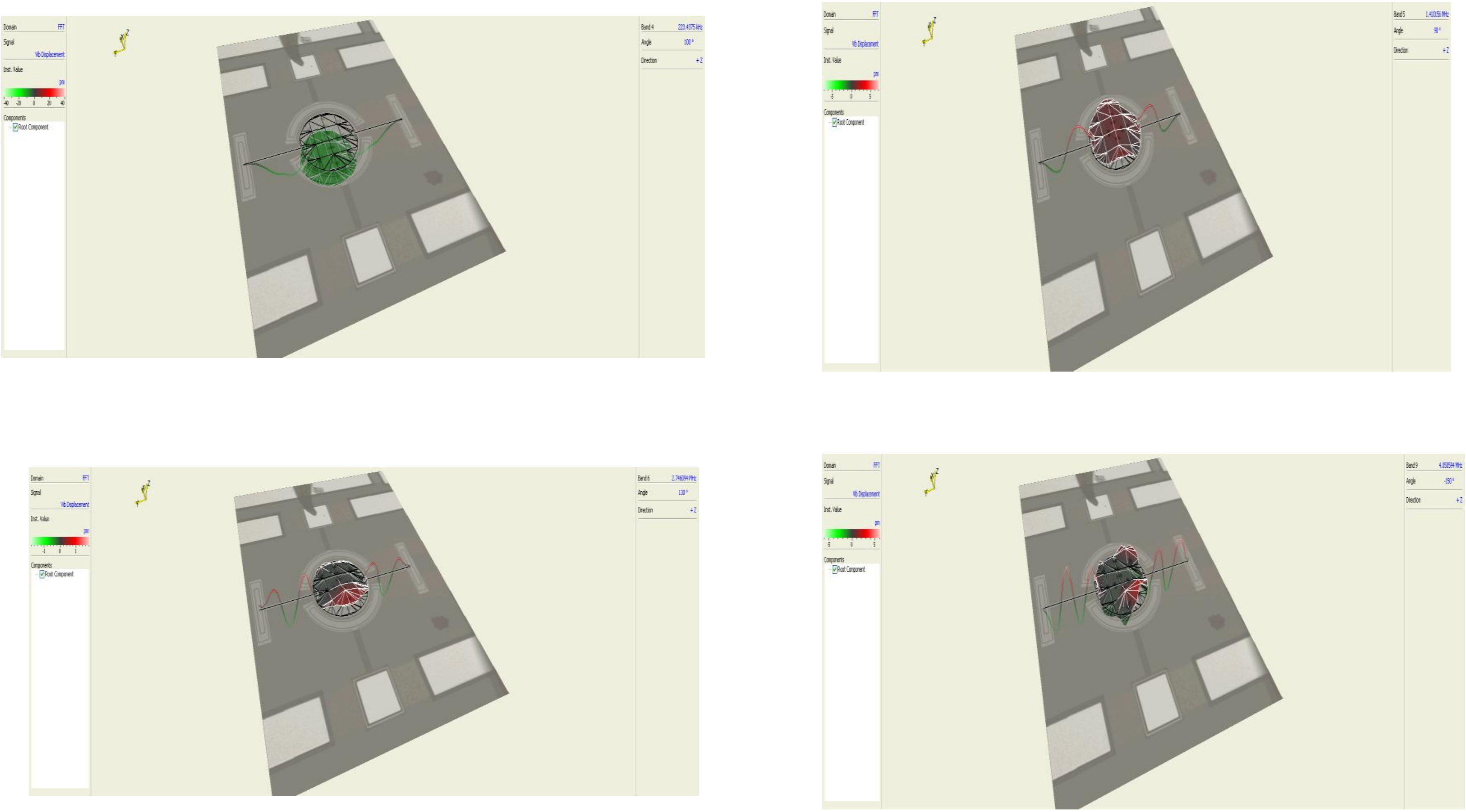

LDV of a side anchored disk resonator

Mechanical Characterization (PBR)

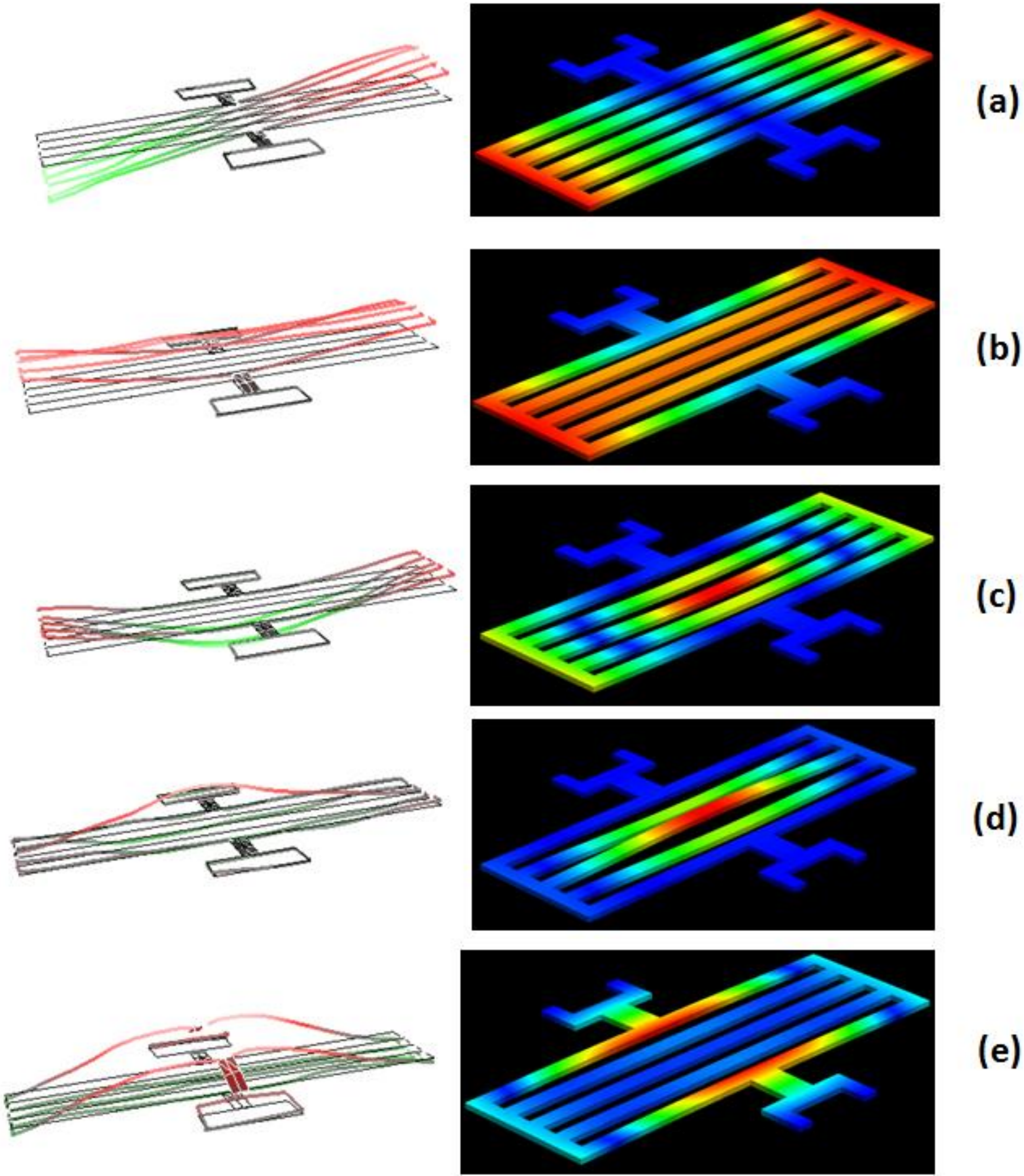

Mechanical Characterization

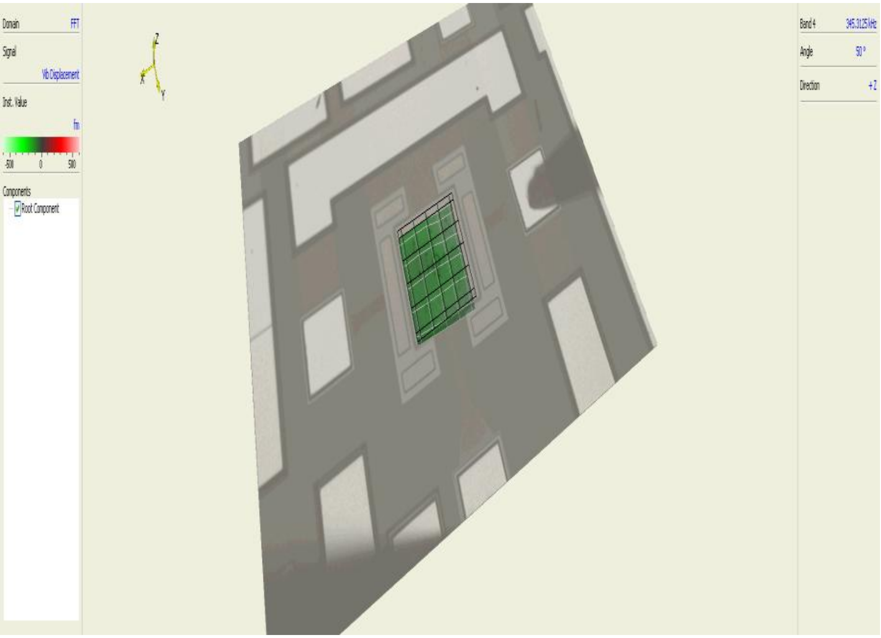

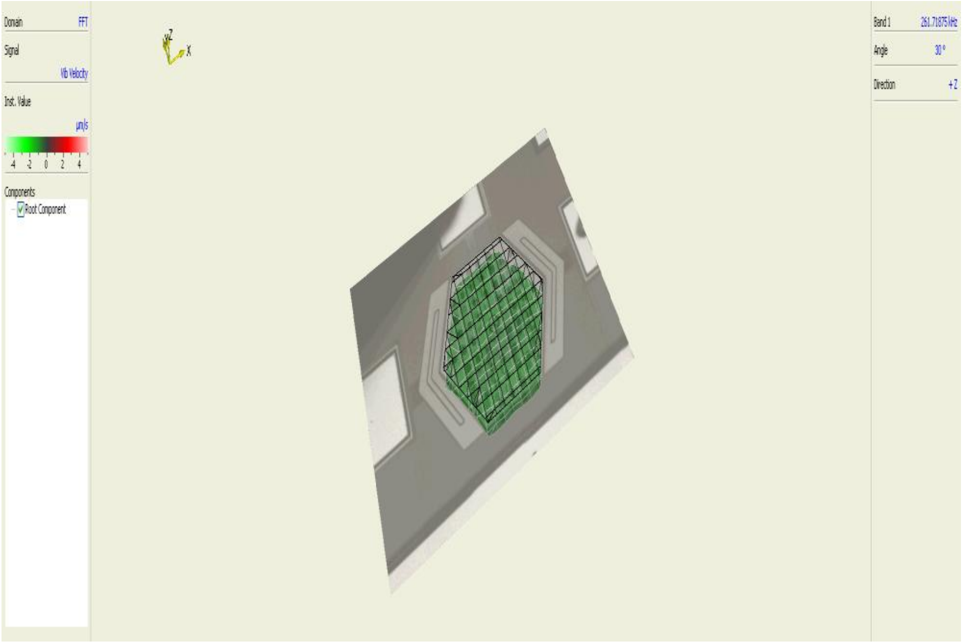

LDV of Square and Hexagonal resonator

Electrical Characterization

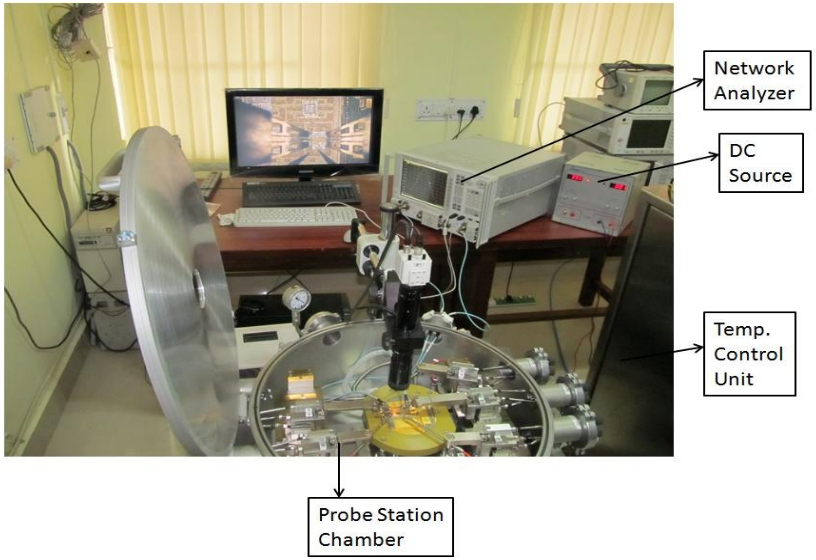

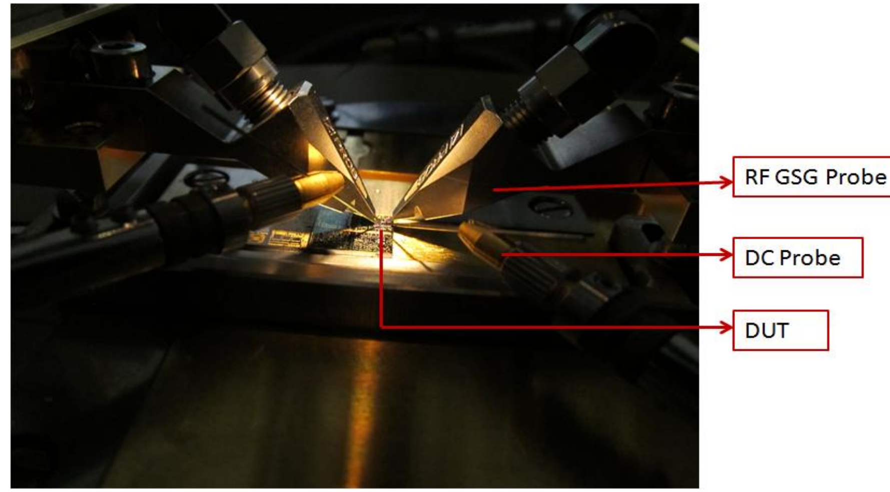

- For the electrical characterization, a typical two-port biasing and excitation scheme was used.

- The fabricated resonators were placed in a RF probe station (Cascade Microtech Inc., USA) and an Agilent network analyzer was used to test their capacitive transduction characteristics.

- dc-bias was applied through the anchors

Nickel Resonators :Transmission Characteristics (air)

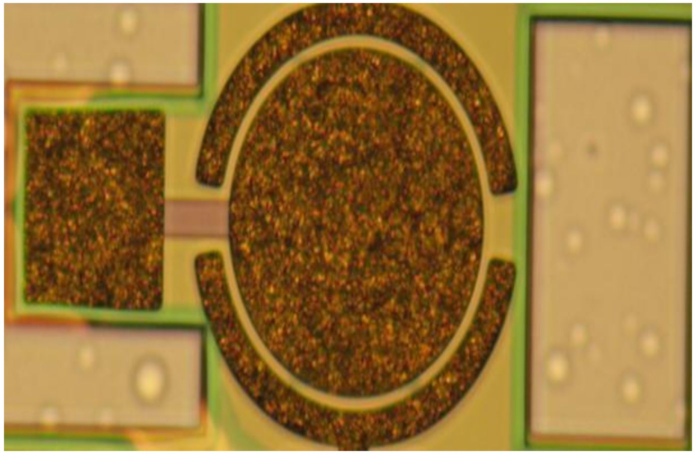

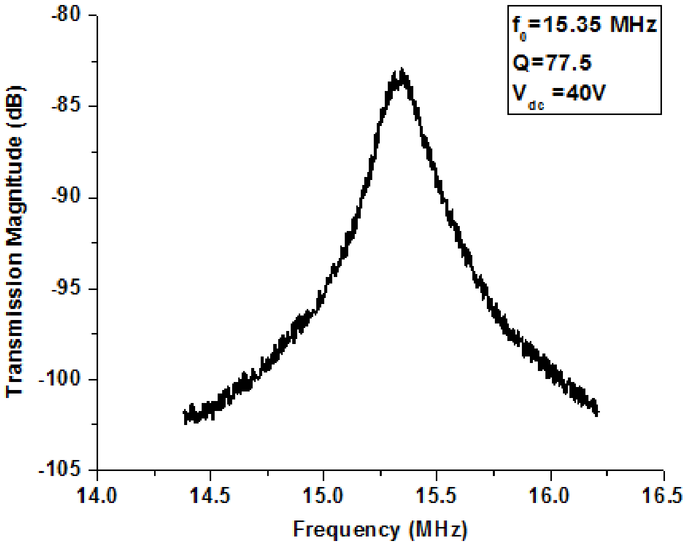

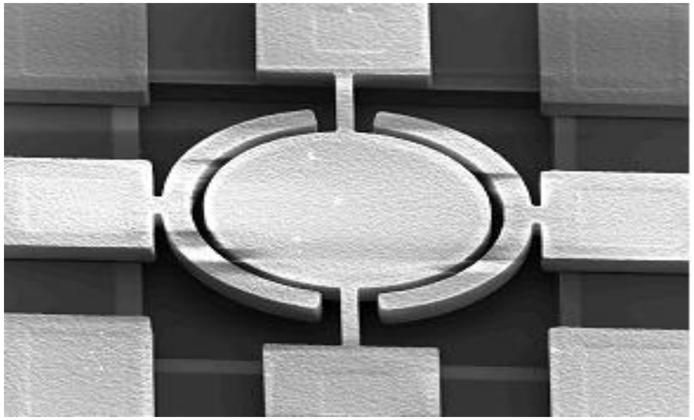

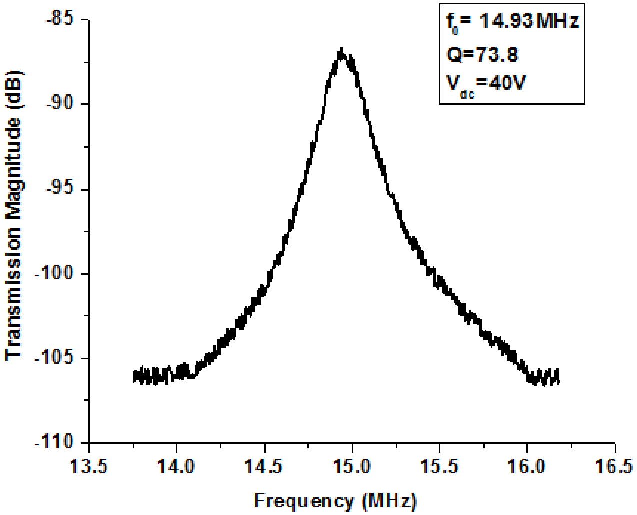

PolysiliconResonators :Transmission Characteristics (air)

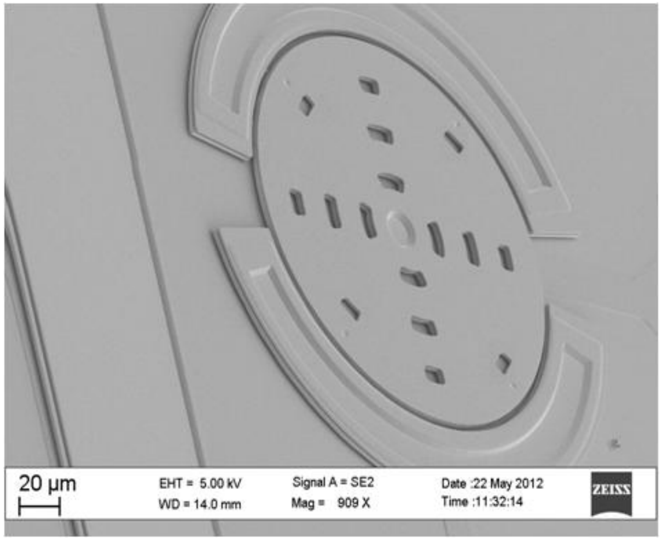

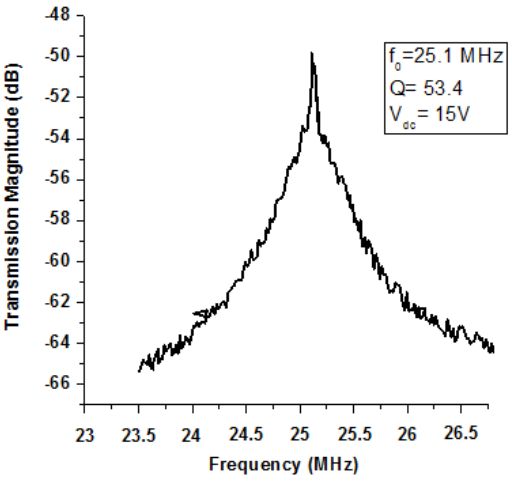

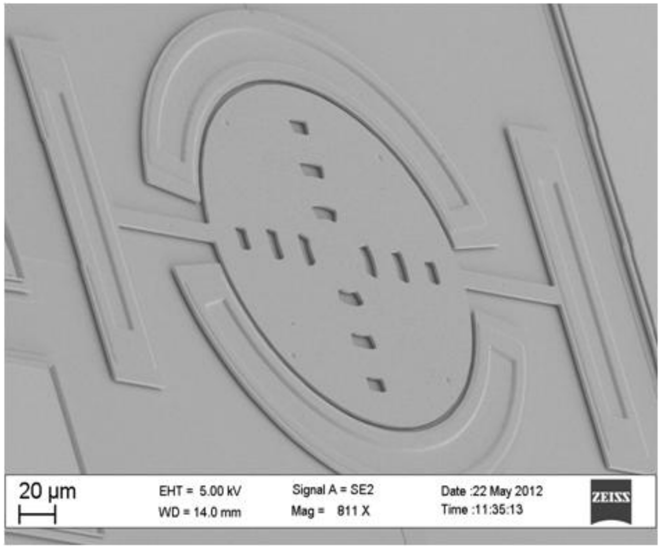

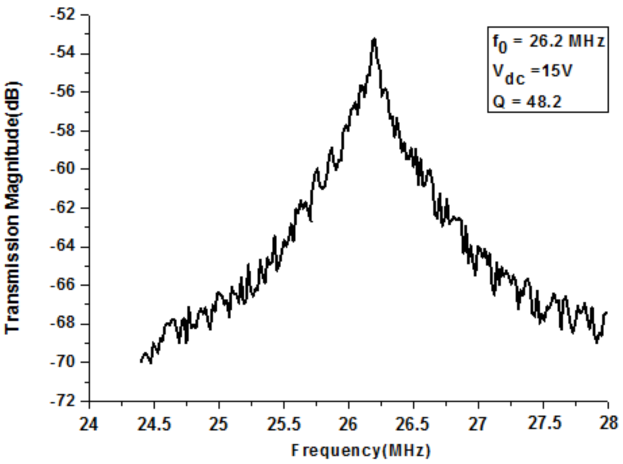

SOI Resonators :Transmission Characteristics (air)

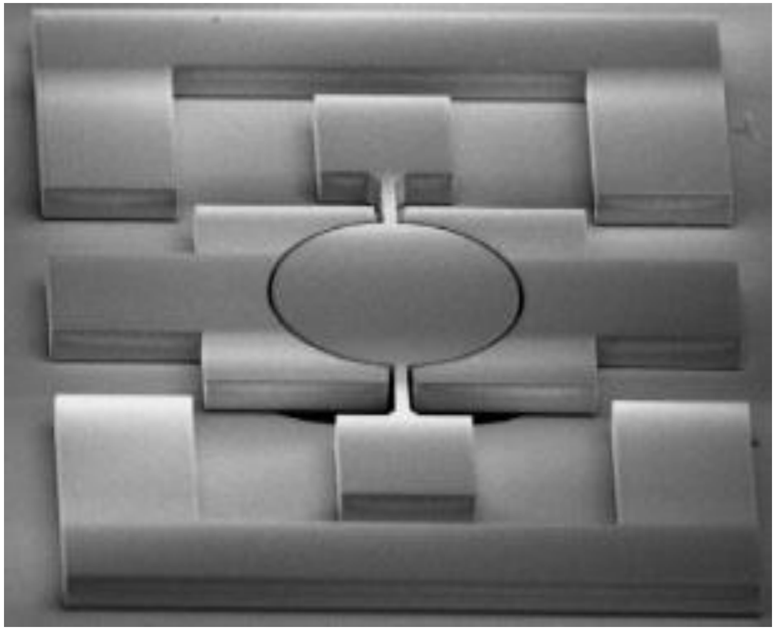

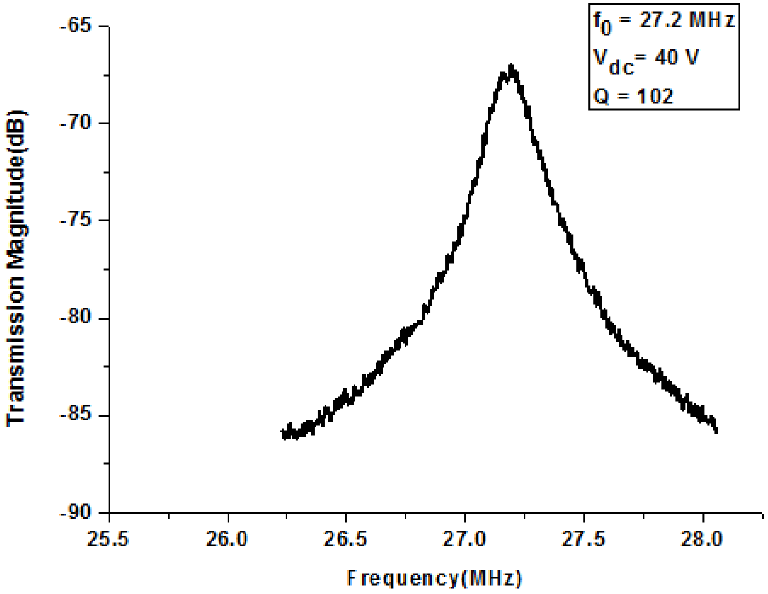

Nickel Resonators :Transmission Characteristics (vacuum)

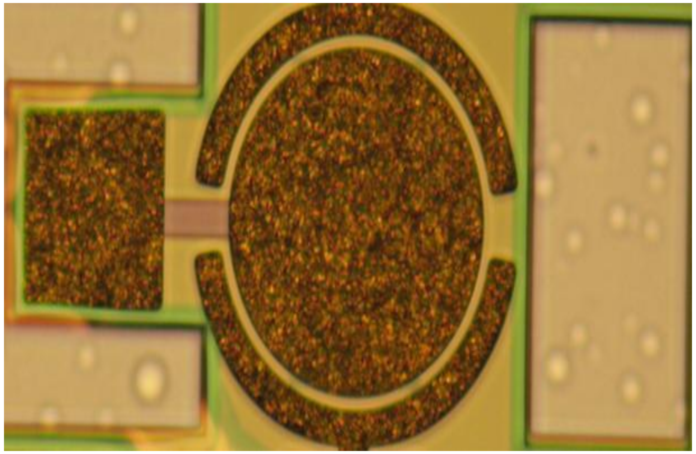

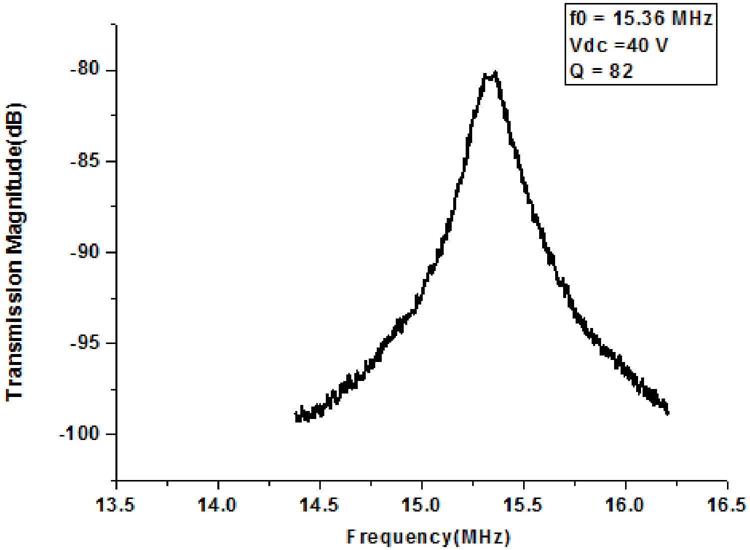

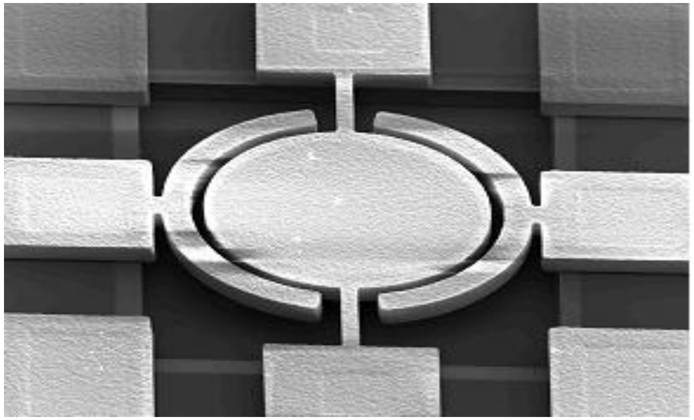

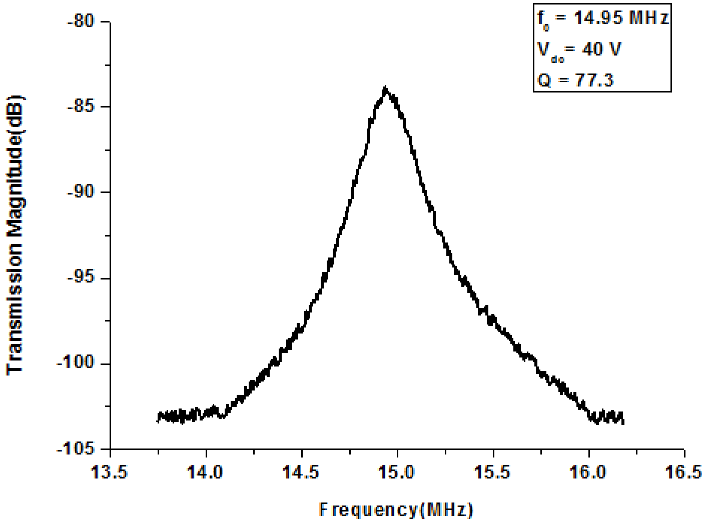

Performance summary of the disk resonators.

Parameter	Poly Si Based bottom anchored disk	Poly Si Based side anchored disk	Ni Based bottom anchored disk	Ni Based side anchored disk	SOI Based side anchored disk
Radius (µm)	99	99	100	100	104
Analytical resonance frequency, f_0. (MHz)	27.12	27.12	15.50	15.50	27.12
Simulated resonance frequency, f_0. (MHz)	27.72	27.71	15.76	15.015	27.93
Measured resonance frequency, f_0. (MHz)	25.1	26.2	15.35	14.93	27.2
Applied dc Bias, V_{dc}.(V)	15	15	40	40	40
Q (simulated)	~68	~62	~101	~96	~123
Q_{Air} (measured)	53.4	48.2	77.5	73.8	102
Q_{vacuum} (measured)	59.7	53.1	82	77.6	116

More

Influence of pressure on Q value

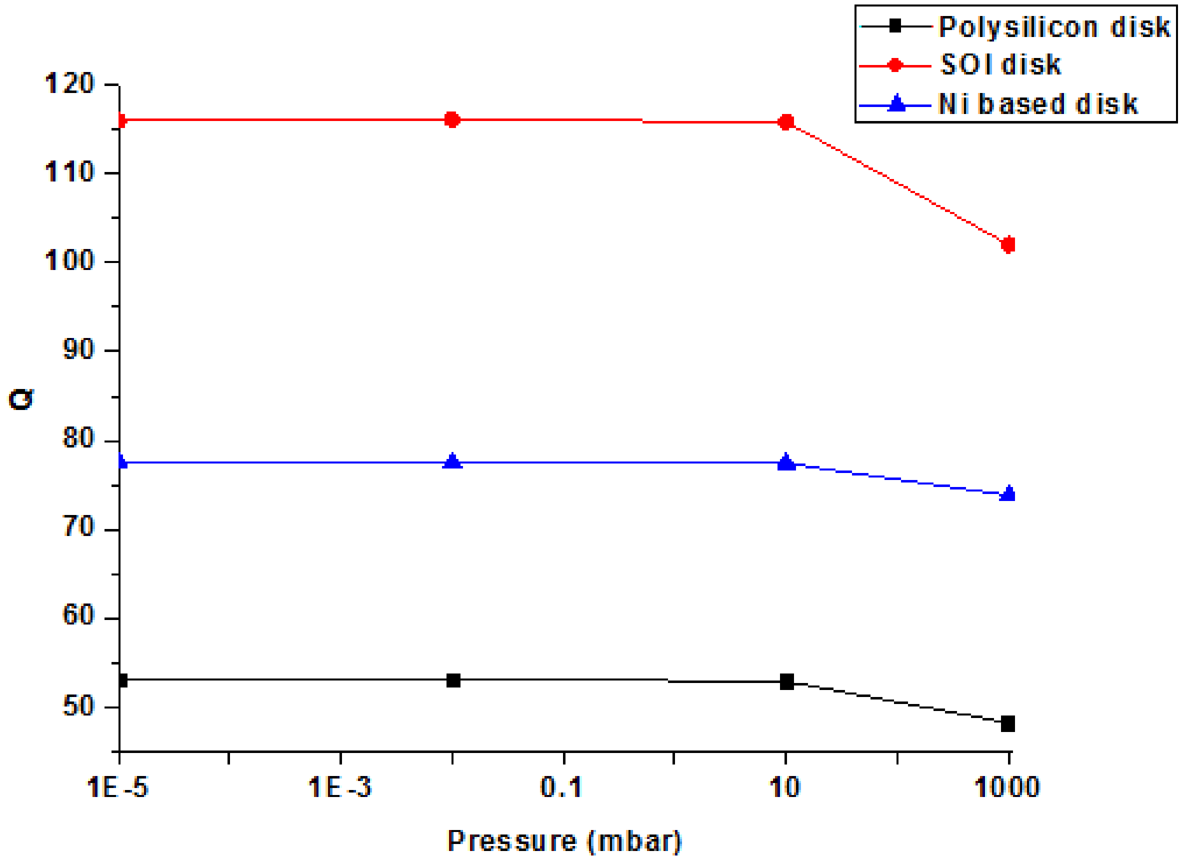

Value of Q factor shows very little change below 10 mbar

Frequency Stability : Temperature dependence

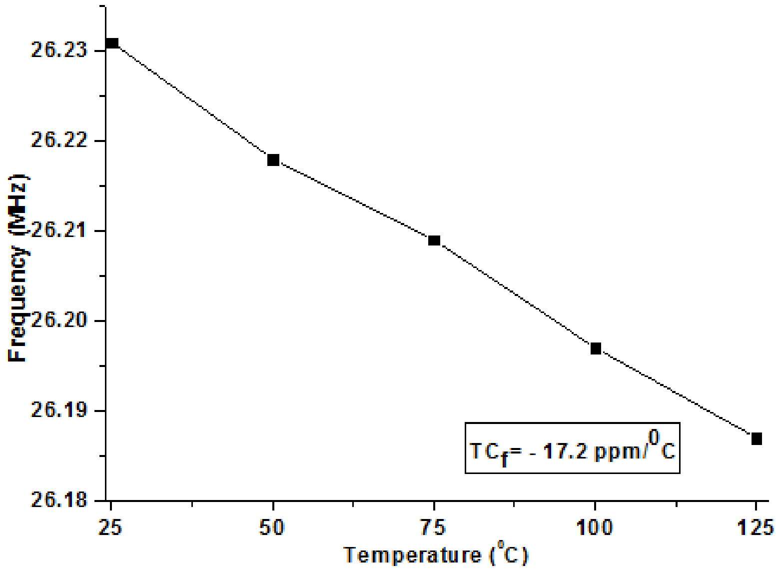

Poly Si

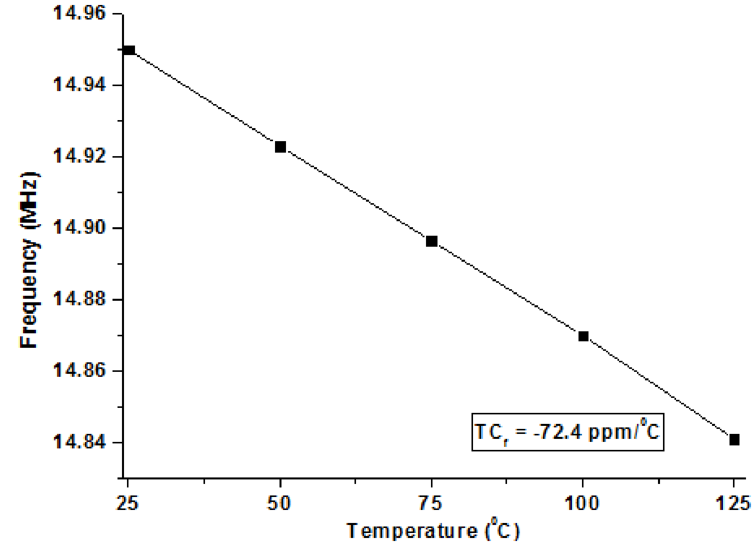

Nickel

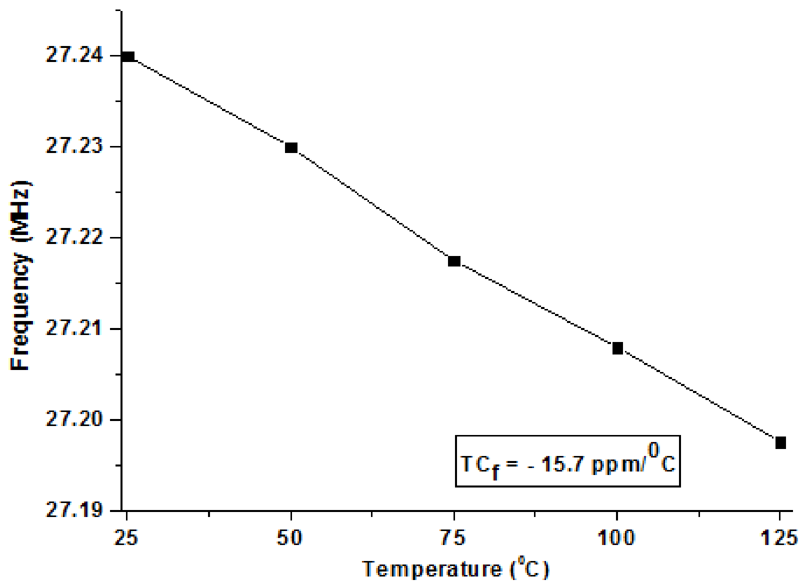

SOI

Frequency Stability : DC bias dependence

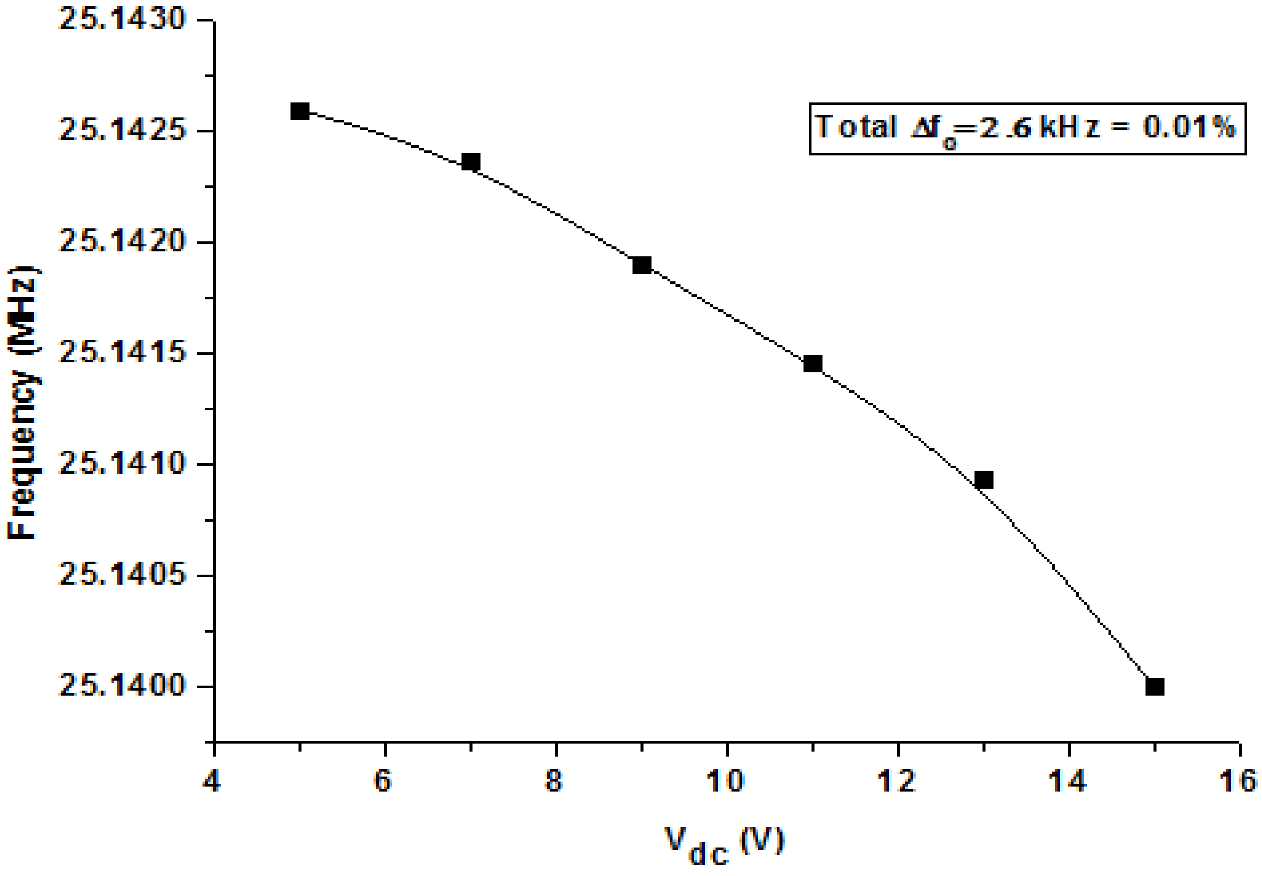

Plot of measured resonance frequency versus DC bias voltage for Polysilicon bottom anchored disk

Performance summary of the alternative extensional mode geometries (Poly Si as structural material)

Parameter	**Longitudinal beam**	**Beam with flanges**	**Parallel beam resonator**	**Square plate resonator**	**Hexagonal plate resonator**
Analytical resonance frequency, f_0. (MHz)	27.12	______	28.9	27.12	27.12
Simulated resonance frequency, f_0. (MHz)	28.09	25.81	29.2	27.83	27.75
Measured resonance frequency, f_0. (MHz)	27.62	25.35	28.89	27.1	25.22
Applied dc Bias, V_{dc}.(V)	15	15	15	15	15
Fabricated Devices	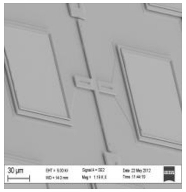	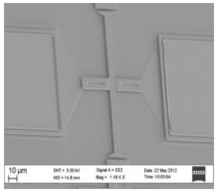	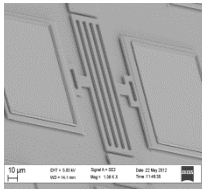	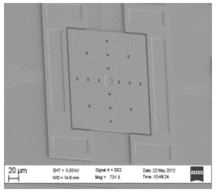	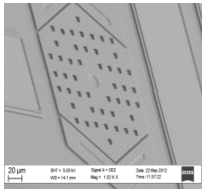
Q_{Air} (measured)	31.5	35.2	39	44.3	61.7

More

Summary : Fabrication processes at a glance

Features	Polysilicon based Process	Nickel based Process	SOI Process
Acoustic Velocity (m/s)	~8300	~4730	~8400
Formation of structural layer	LPCVD	Electroplating	Etching of SOI wafers
Deposition Temperature (^{0}C)	~ 600 ^{0}C	~ 50 ^{0}C	_______
Transduction Gap (µm)	3	9	3
Thickness of the structural layer (µm)	2	20.5	25
Fabricated Devices	 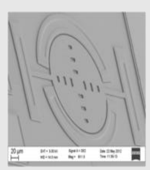	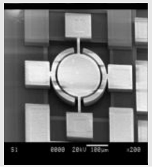 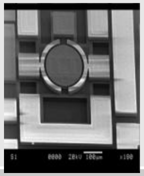	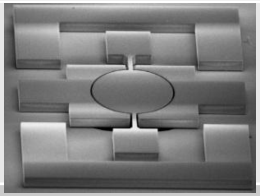
Q (Air)	53.4 48.2	73.8 77.5	102
Q (Vacuum)	59.7 53.1	77.5 82	116

Disk Resonator-based BPF

Entity	Value
Disk radius (R)	50 µm
Disk and coupler thickness (t)	2.0 µm
Stem radius (r)	2.0 µm
Coupler length (L_s)	38.5 µm
Coupler width (W_s)	2.98 µm
Resonator spring constant (k_r)	3.150e6 N/m
Coupler spring constant (K_{sij})	3.83246e4 N/m
Resonance frequencies	54.303, 54.758 & 55.252 MHz

Some parameters of a PolyMUMPs based BPF

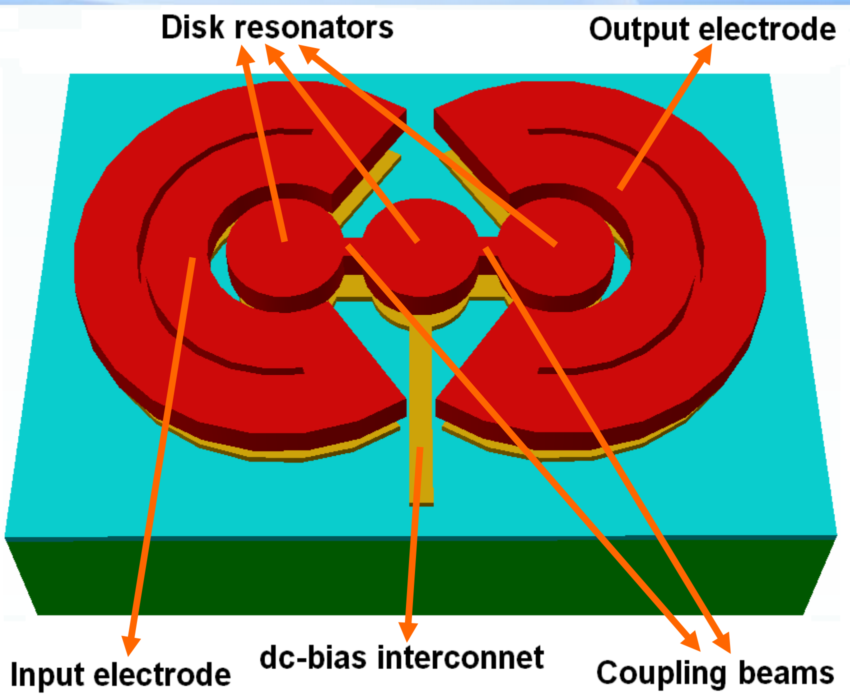

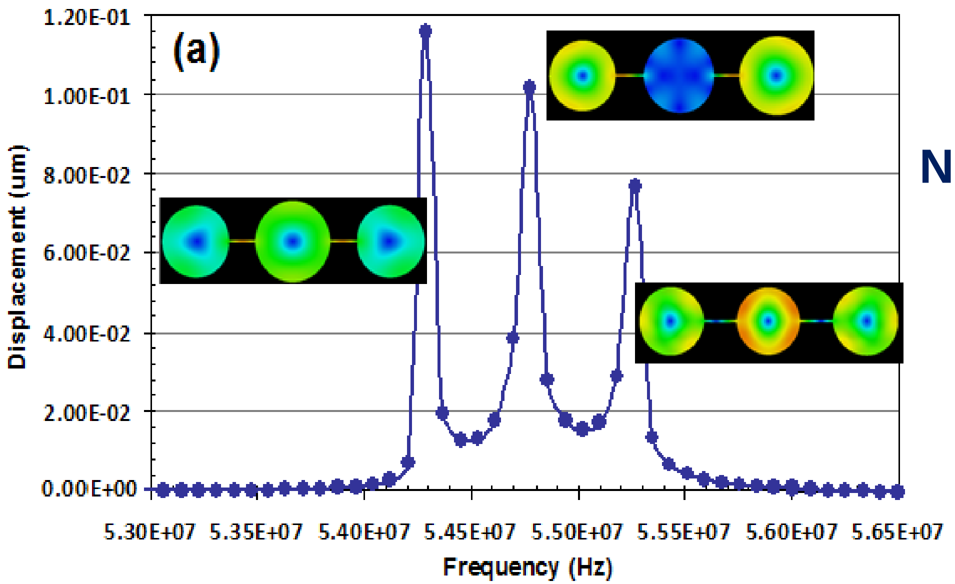

No. of modes = no. of coupled resonators

Un-terminated harmonic response of triple disk BPF

Disk Resonator-based BPF : Vertical Stacking

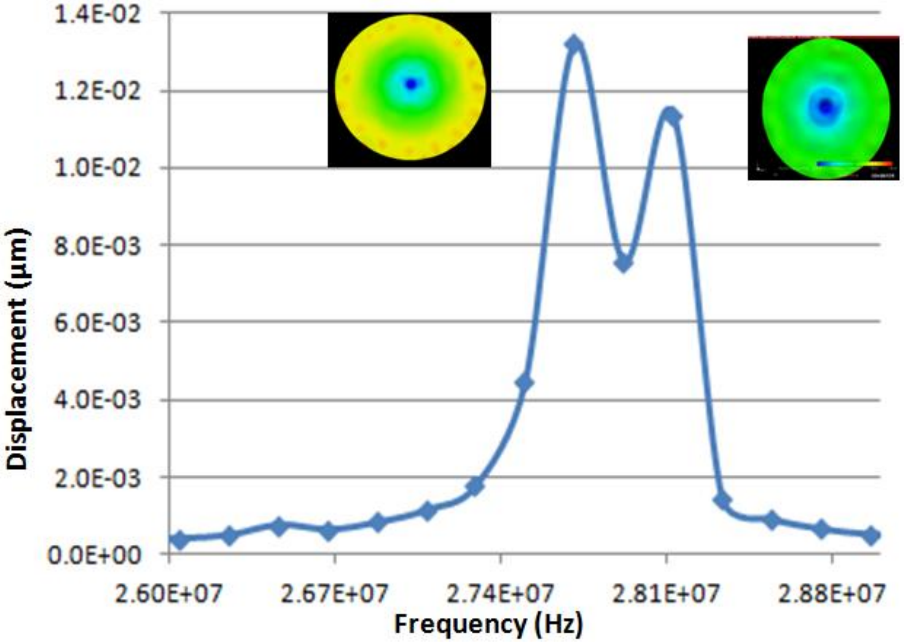

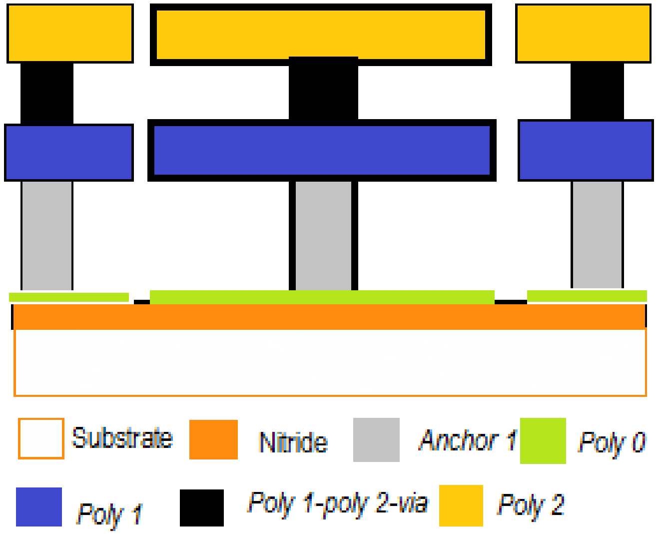

Entity	Value
Disk Radius	99 µm
Thickness of the upper disk	1.5 µm
Thickness of the lower disk	2.0 µm
Height of the coupling stem	0.75 µm
Height of the bottom anchor	2.0 µm
Disk to electrode gap	3.0 µm
Resonance frequencies	27.654 & 28.068 MHz

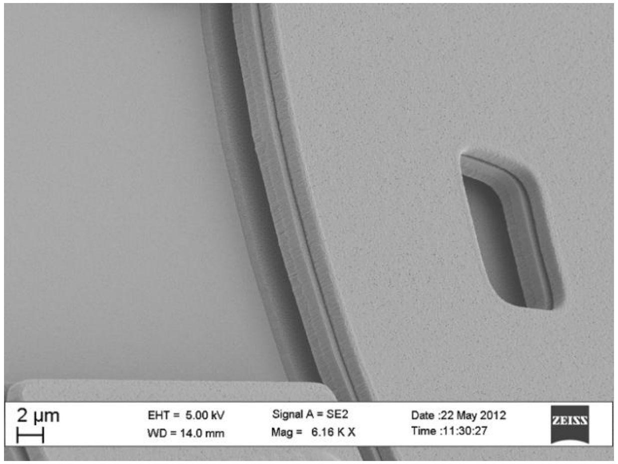

Conclusions

1. MEMS based radial contour mode disk resonators using surface micromachined poly silicon, electroplated nickel and single crystal silicon (SOI) as structural material were developed. Electrical, material and mechanical characterization of the structures were carried out to analyze their functionality.

2. Different extensional mode resonator geometries using polysilicon as structural material were fabricated and characterized. Among them, Hexagonal plate extensional mode geometry provides a better alternative to the disk resonators.

3. Performance comparison of the disk resonators realized using different structural material was done. Disk resonators fabricated using SOI (Silicon-on-Insulator) process which has larger structural layer thickness (25µm) and transduction gap (3µm) comparable to the Polysilicon process results in improved performance.

4. Feasibility of electrodeposited nickel as a low cost CMOS compatible MEMS functional layer has been studied extensively.

5. Attempt was made to develop disk resonator based filter design as a proof of concept.

Future Work :Resonators with higher resonance frequency

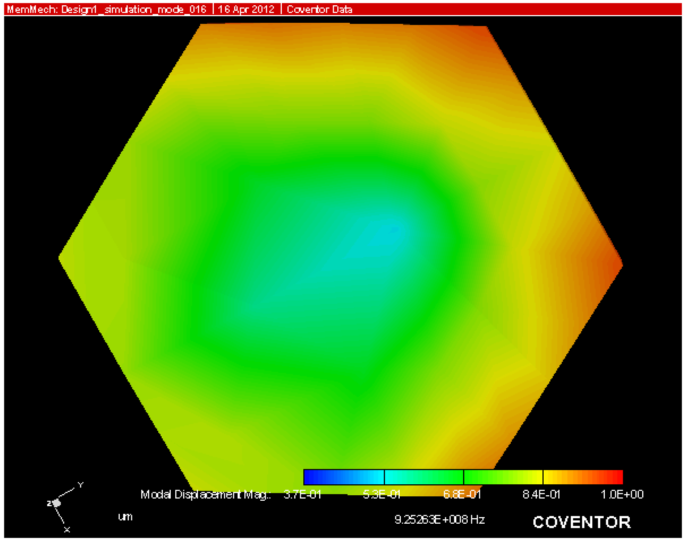

Hexagonal resonator with f_0 = 915 MHz

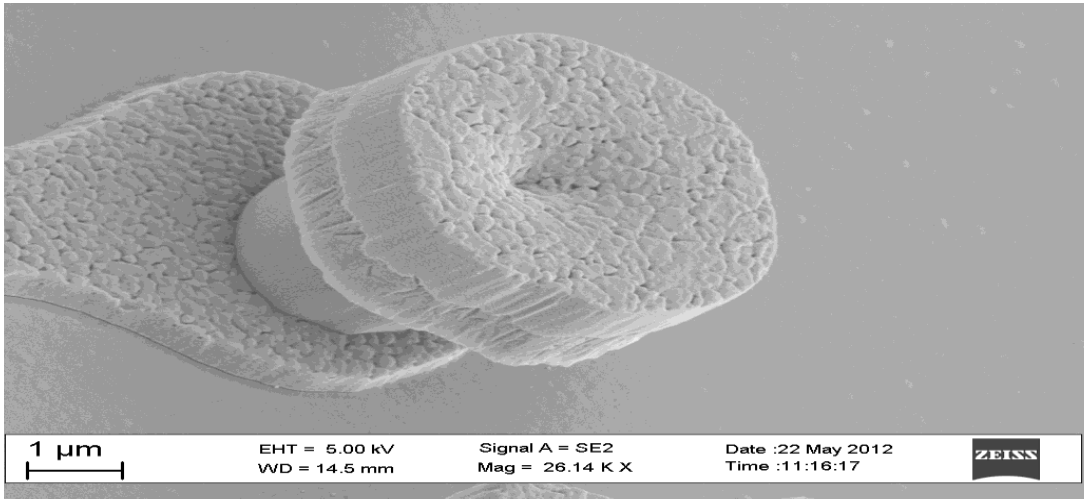

MEMS on top of CMOS: SiGe MEMS

Process information:

- The SiGeMEMS process can be processed on top of previously processed CMOS wafers.
- Poly-SiGe is used as structural material.
- 500 nm horizontal gaps can be achieved for capacitive devices

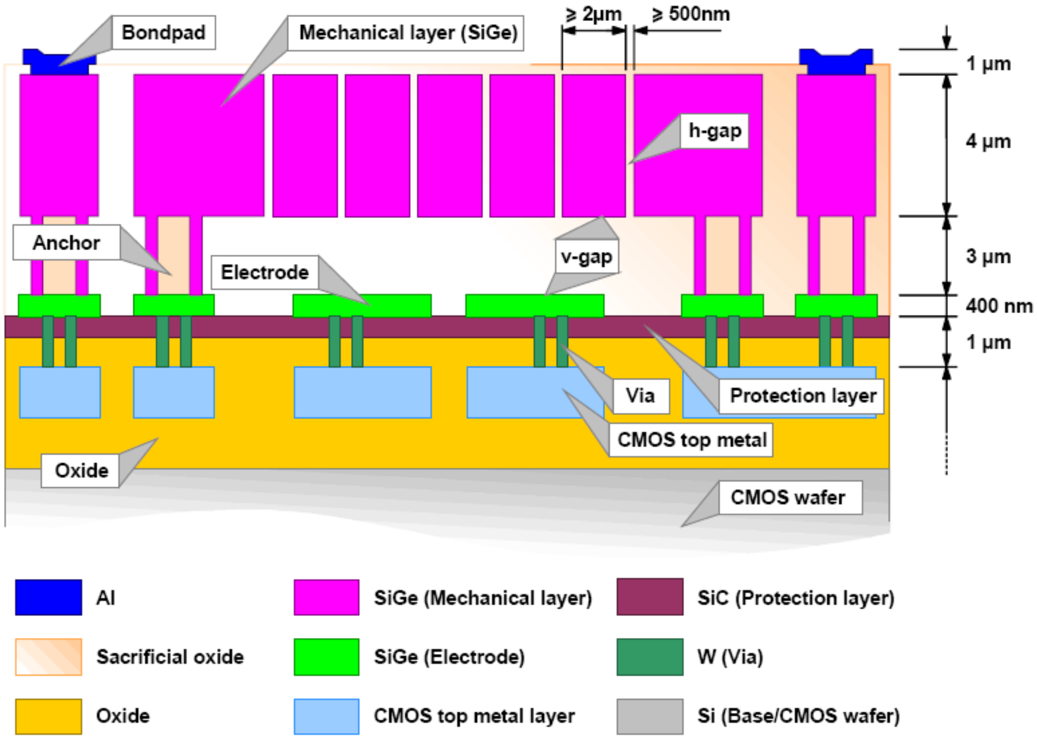

Fig: Schematic cross section of the SiGeMEMS process indicating materials, functional parts and the main dimensional features

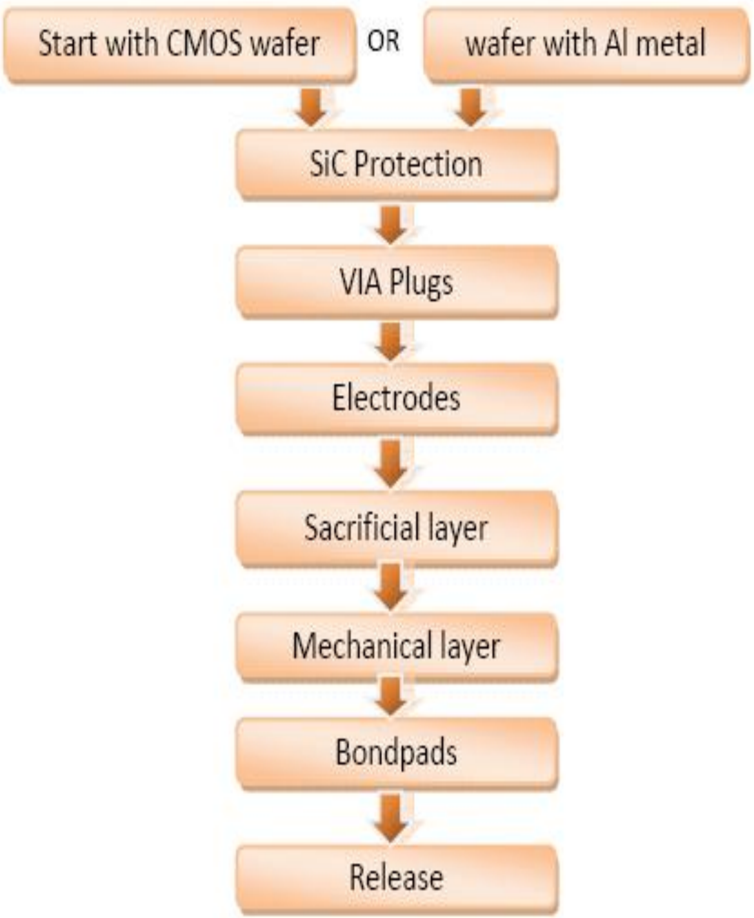

Fig: Schematic process flow

Future Work : Nano resonators

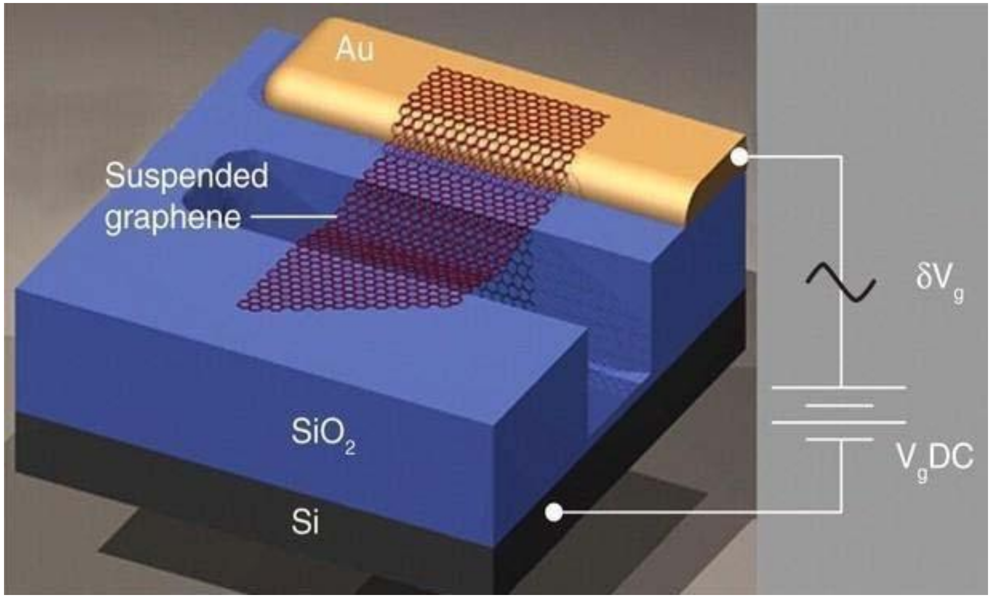

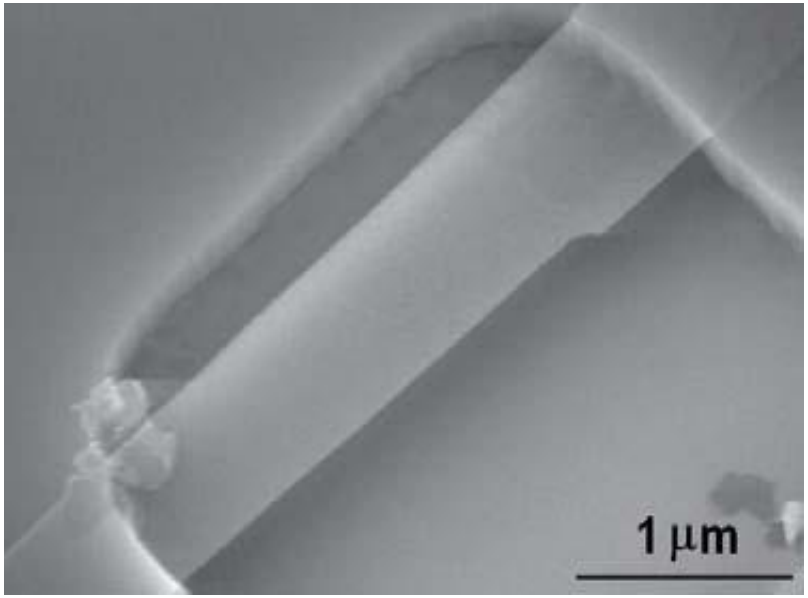

Schematic diagram (a) and SEM (b) of a suspended graphene resonator

Bibliography

C.T.C Nguyen, “Frequency selective MEMS for miniaturized low-power communication devices,” *IEEE Trans. Microwave Theory Tech.*,Vol.47,pp.1486-1503,1999.

J. Wang, Z. Ren, and C. T.-C. Nguyen, “1.156-GHz self-aligned vibrating micromechanical disk resonator,” *IEEE Transactions on Ultrasonics, Ferroelectrics and Frequency Control*, vol. 51, pp. 1607–1628, December 2004.

C. T.C. Nguyen, “MEMS Technology for Timing and Frequency Control,” *IEEE Transactions on Ultrasonics, Ferroelectrics and Frequency Control*, vol. 54, no.2, pp.251– 270, February 2007.

Y.-W. Lin, S. Lee, S.-S. Li, Y. Xie, Z. Ren, and C. T.-C. Nguyen, “Seriesresonant VHF micromechanical resonator reference oscillators,” *IEEE Journal of Solid-State Circuits*, vol. 39, pp. 2477–2491, 2004.

S. Lucyszyn, “Review of radio frequency microelectromechanical systems technology,” *IEE Proceedings- Science, Measurement and Technology*, vol. 151, pp. 93–103, 2004.

J. R. Clark, W. -T. Hsu, M. A. Abdelmoneum, and Clark T.-C. Nguyen, “High-Q UHF Micromechanical Radial-Contour Mode Disk Resonators,” *Journal of Microelectromechanical Systems*, vol. 14, no. 6, pp. 1298–1310, 2005.

R. T. Howe and R. S. Muller, “Polycrystalline silicon micromechanical beams,” *Journal of the Electrochemical Society*, vol. 130, pp. 1420–1423, 1983.

F. D. Bannon, J. R. Clark and C. T. C. Nguyen, “High frequency micromechanical filters,” *IEEE Journal of Solid-State Circuits*, vol. 35, pp. 512–526, 2000.

Y. -W. Lin, S. Lee, S. -S. Li,Y. Xie, Z. Ren, and C.T.-C. Nguyen, “Series resonant VHF micromechanical resonator reference oscillators,” *IEEE Journal of Solid-State Circuits*, vol. 39, no. 12, pp. 2477–2491, 2004.

S. Pourkamali, A. Hashimura, R. Abdolvand, G. K. Ho, A. Erbil, and F. Ayazi, “High-Q single crystal silicon HARPSS capacitive beam resonators with selfaligned sub-100-nm transduction gaps,” *Journal of Microelectromechanical Systems*, vol. 12, no. 4, pp. 487–496, 2003.

K. Wang, A.-C. Wong and C. T.-C. Nguyen, “VHF free-free beam high-Q micromechanical resonators,” *Journal of Microelectromechanical Systems*, vol. 9, no. 3, pp. 347–360, 2000.

W. C. Tang, T.-C. H. Nguyen, and R. T. Howe, “Laterally driven polysilicon resonant microstructures,” *Proceedings of the IEEE Micro Electro MechanicalSystems*, Salt Lake City, Utah, February 1989, pp. 53–59.

K. R. Cioffi and W.-T. Hsu, “32 KHz MEMS-based oscillator for low-power applications,” *Proceedings of the 2005 IEEE International Frequency Control Symposium and Exposition*, Vancouver, Canada, August 2005, pp.551–558.

J. E.-Y. Lee, B. Bahreyni, Y. Zhu, and A. A. Seshia, “A Single-Crystal-Silicon Bulk-Acoustic-Mode Microresonator Oscillator,” *IEEE Electron Device Letters*, vol. 29, no. 7, pp. 701–703, 2008.

S. A. Bhave, G. Di, R. Maboudian, and R.T. Howe, “Fully-differential poly-SiC Lame mode resonator and checkerboard filter,” *Proceedings of the 18th IEEE International Conference on Micro Electro Mechanical Systems*, Miami, FL, January–February 2005, pp. 223–226.

Y.-W. Lin, S. Lee, S.-S. Li, Y. Xie, Z. Ren, and C. T.-C. Nguyen, “60-MHz wine glass micromechanical disk reference oscillator,” *Digest of Technical Papers of the 2004 IEEE International Solid-State Circuits Conference*, San Francisco, CA, February 2004, pp. 322–323.

J.E.-Y. Lee and A.A. Seshia, “5.4-MHz single-crystal silicon wine glass mode disk resonator with quality factor of 2 million,” *Sensors and Actuators A*, vol. 156, 28–35, 2009.

J. R. Clark, W.-T. Hsu, M. A. Abdelmoneum, and C. T.-C. Nguyen, “High-Q UHF Micromechanical Radial-Contour Mode Disk Resonators,” *Journal of Microelectromechanical Systems*, vol. 14, pp. 1298–1310, 2005.

Huang W.L, Ren Z, Lin Y.W, Chen H.Y, Lahann J, Nguyen C.T.C, “Fully monolithic CMOS nickel micromechanical resonator oscillator,” *In: Proceedings of the 21st IEEE international conference on microelectromechanical systems*, Tucson, Arizona, pp 10–13,2008.

List of publications

Journal:

1. **Ritesh Ray Chaudhuri** and Tarun K. Bhattacharyya, “Electroplated nickel based micro-machined disk resonators for high frequency applications” *Microsystem Technologies,* vol. 19(4), pp. 525-535, 2013.
2. **Ritesh Ray Chaudhuri** and Tarun K. Bhattacharyya, “Design and fabrication of micromachined polysilicon resonators,” *Journal of ISSS (under review).*

Conference:

1. **Ritesh Ray Chaudhuri** and Tarun K. Bhattacharyya, “Microelectromechanical Longitudinal Beam Resonator for Frequency Reference Applications*” 26th International Conference on VLSI Design*, Pune, 2013.

2. **Ritesh Ray Chaudhuri**, Joydeep Basu and Tarun Kanti Bhattacharyya, “Design and Fabrication of Micromachined Resonators.” *Sixth International Conference on Smart Materials Structures and Systems (ISSS)*, Bangalore, 2012.

3. Joydeep Basu**, Ritesh Ray Chaudhuri**, Anindya lal Roy and Tarun Kanti Bhattacharyya, “A Microelectromechanical Disk Resonator-based Bandpass Filter for Wireless RF Applications*.” IEEE Applied Electromagnetics Conference*, Kolkata, 2011.

Thank You . . .

Appendix A

$$\left(\frac{\zeta}{\xi}\right)\frac{J_0(\zeta/\xi)}{J_1(\zeta/\xi)} = 1-\sigma \qquad (1)$$

Where

$$\zeta = 2\pi f_0 R\sqrt{\frac{\rho(2+2\sigma)}{E}} \qquad (2)$$

$$\xi = \sqrt{\frac{2}{1-\sigma}} \qquad (3)$$

$$\lambda_i \frac{J_0(\lambda_i)}{J_1(\lambda_i)} = 1-\sigma \qquad (4)$$

$$f_0 = \frac{\lambda_i}{2\pi R}\sqrt{\frac{E}{\rho(1-\sigma^2)}} \qquad (5)$$

Back

Appendix B

Mode number (i)	Value of frequency parameter (λ_i) for Nickel	Value of frequency parameter (λ_i) for PolySilicon	Value of frequency parameter (λ_i) for single crystal silicon
1	2.06	1.99	2.05
2	5.4	5.37	5.39
3	8.58	8.42	8.58
4	11.74	11.52	11.74

Appendix C: Mechanical Model

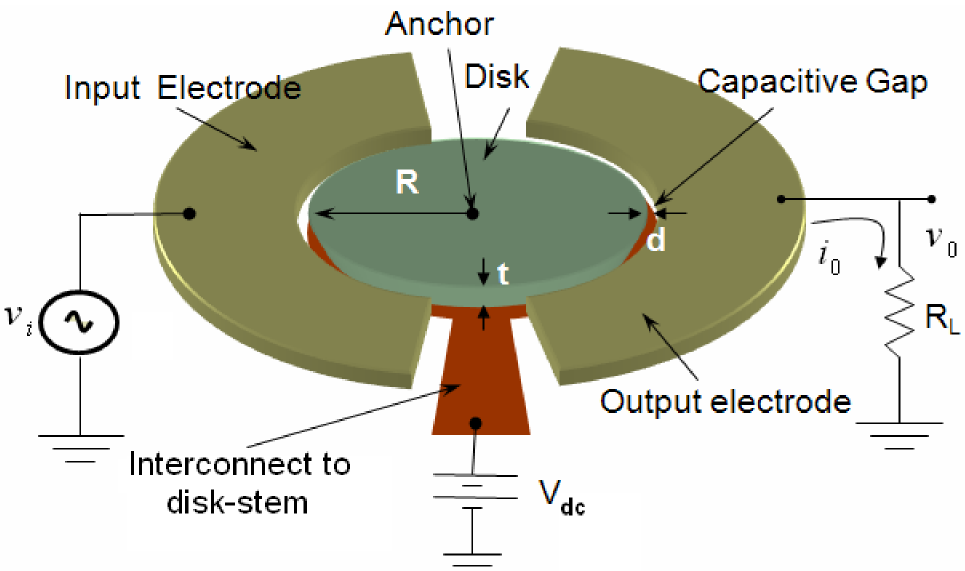

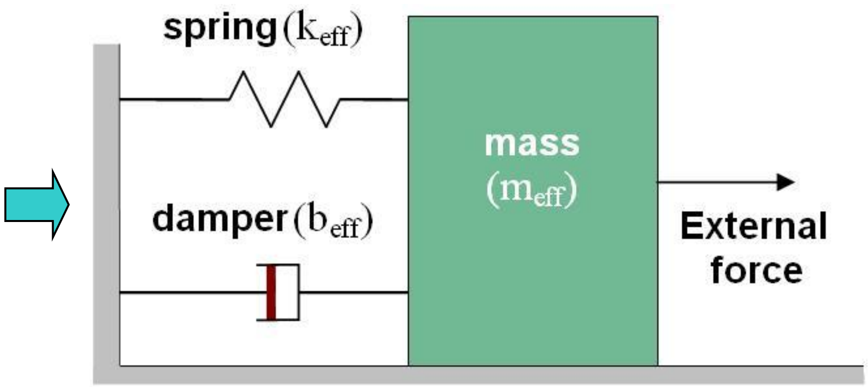

$$m_{eff} = \frac{2E_k}{v^2(R)} = \frac{2\pi\rho t\int_0^R r\,J_1(hr)^2\,dr}{J_1(hR)^2} = \pi\rho t R^2\left[1 - \frac{J_0(hR)J_2(hR)}{J_1(hR)^2}\right]$$

$$\text{with, } h = \omega_0\sqrt{\frac{\rho}{\left(\frac{E}{1+\sigma}\right)+\left(\frac{E\sigma}{1-\sigma^2}\right)}} = \frac{\lambda_i}{R}$$

$$\omega_0 = \sqrt{k_{eff}/m_{eff}}$$

$$b_{eff} = \frac{\omega_0 m_{eff}}{Q} = \frac{\sqrt{k_{eff}m_{eff}}}{Q}$$

Appendix D

- **Disk Resonators: Electrical Model**

$$\begin{bmatrix} i_0 \\ v_i \end{bmatrix} = \begin{bmatrix} 0 & n \\ \frac{1}{n} & 0 \end{bmatrix} \begin{bmatrix} F \\ \dot{r} \end{bmatrix}$$

$$n_k = V_{dc}\frac{\partial C_k}{\partial r} = V_{dc}\frac{\partial}{\partial r}\left(\frac{\varepsilon A_k}{d_0 - r}\right) \approx V_{dc}\left(\frac{\varepsilon A_k}{d_0^2}\right) \quad (\text{for, } r << d)$$

$$L_e = \left(\frac{l_e}{n^2}\right)$$

$$C_e = (n^2 c_e)$$

$$R_e = \left(\frac{r_e}{n^2}\right)$$

$$R_e = \left(\frac{1.18 \times 10^{29}}{Q V_{dc}{}^2}\right)\left(\frac{d^4}{Rt}\right)$$

Back

Appendix E

Structural response of the disk resonator subjected to a harmonic excitation:

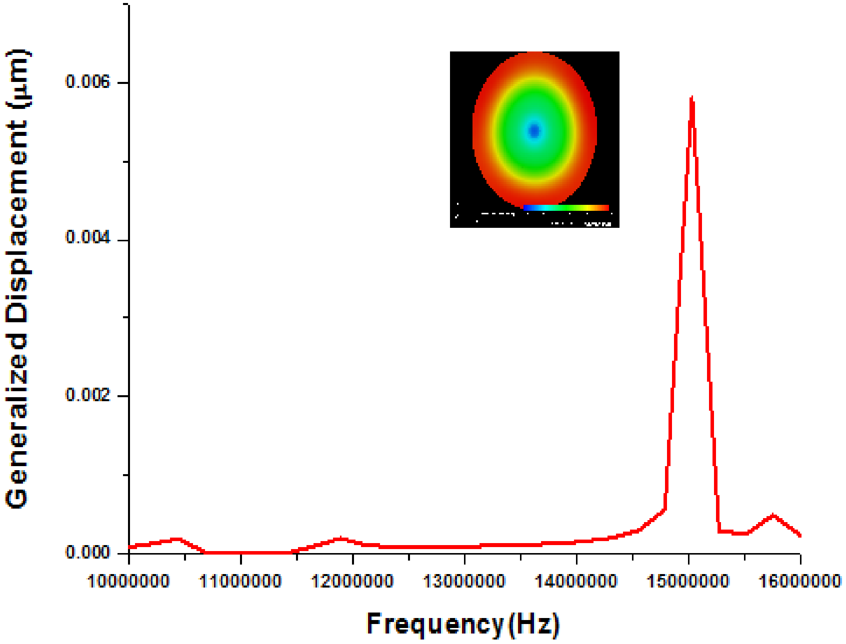

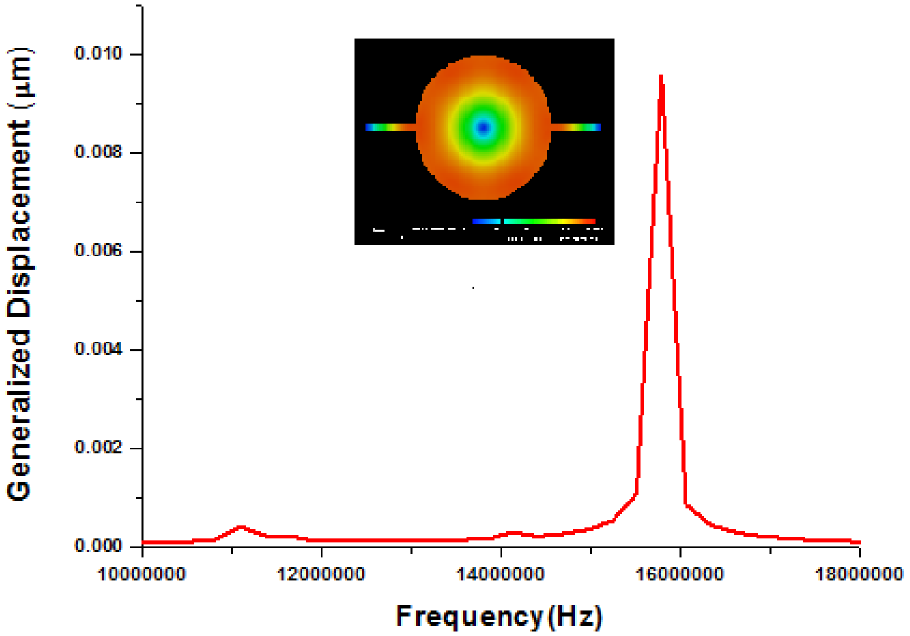

Appendix E

Structural response of the disk resonator subjected to a harmonic excitation:

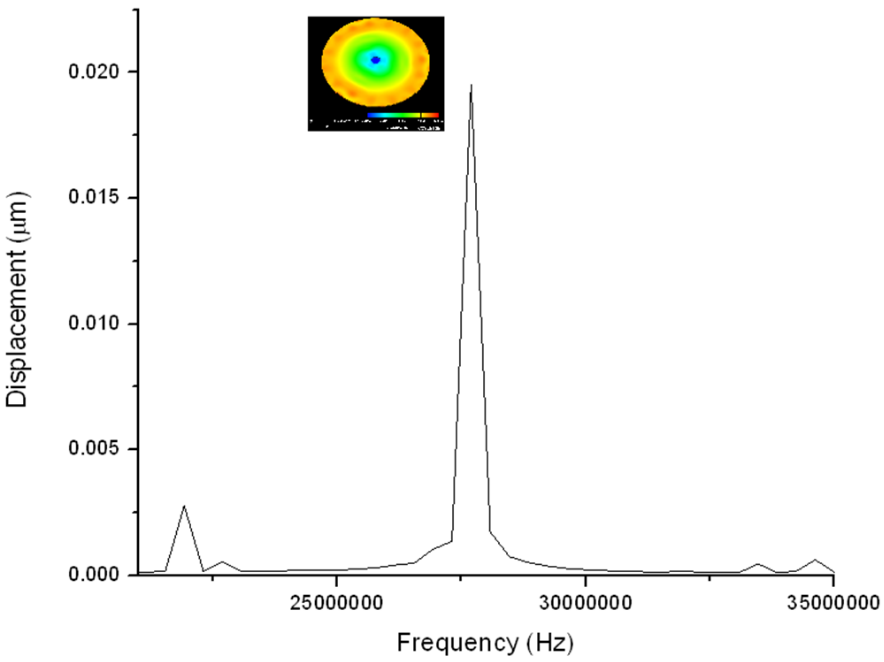

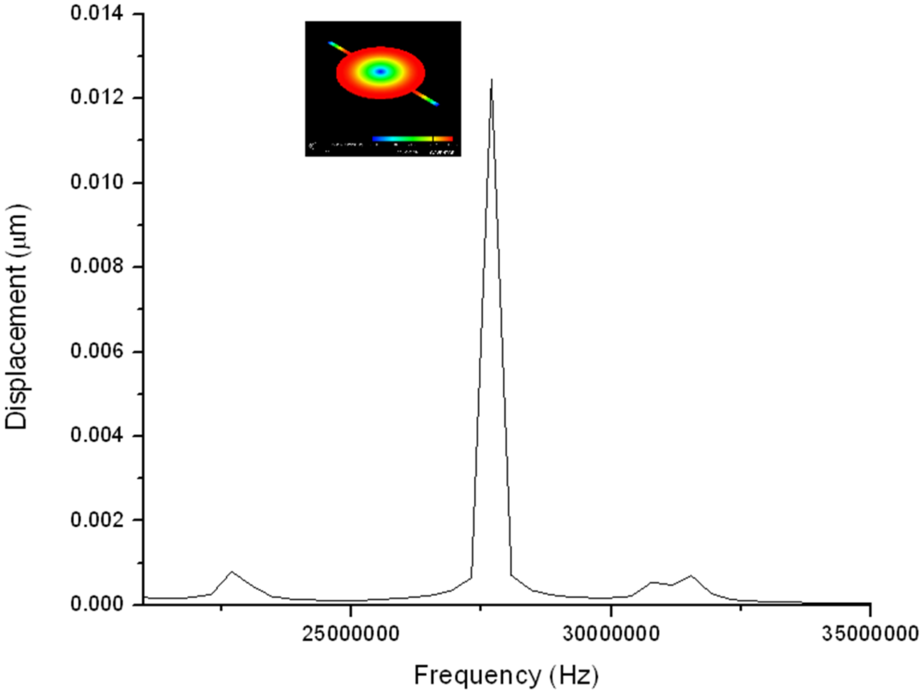

Back

Appendix F

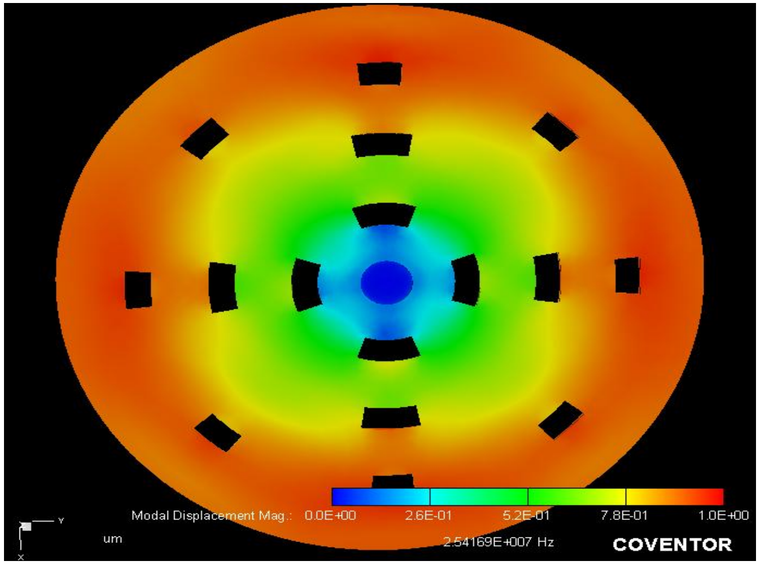

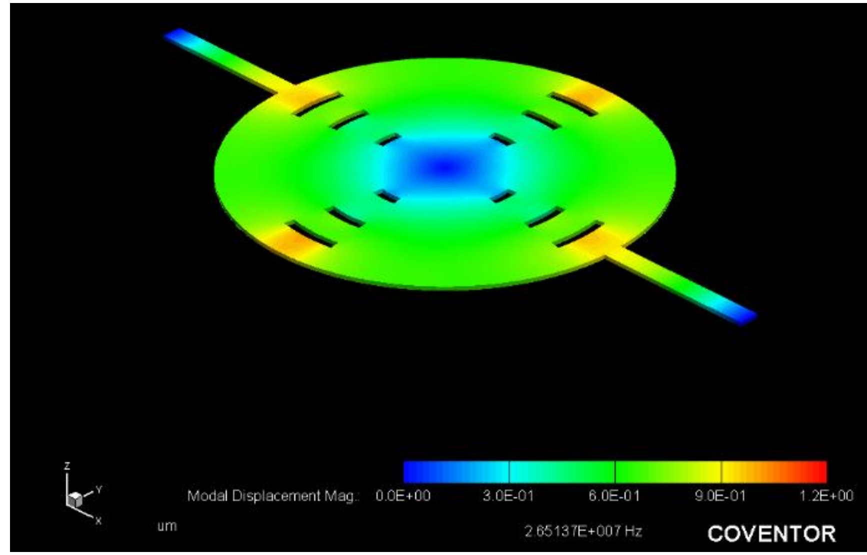

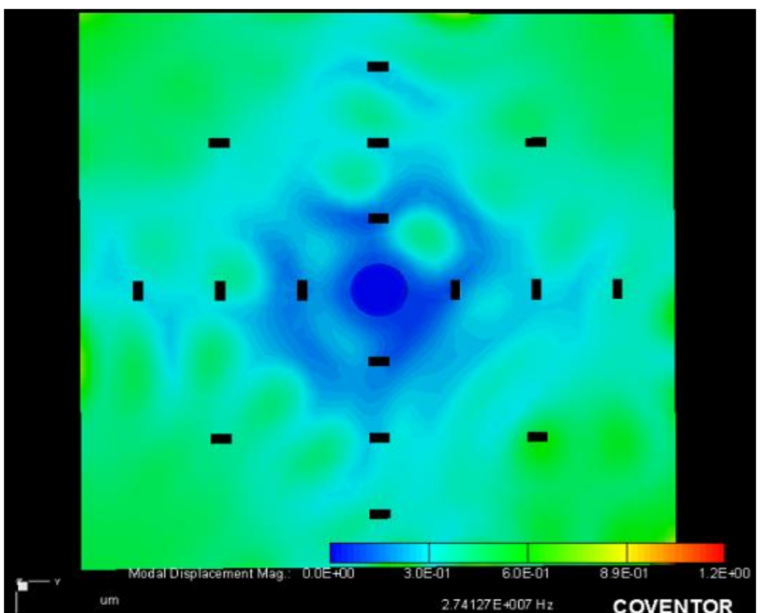

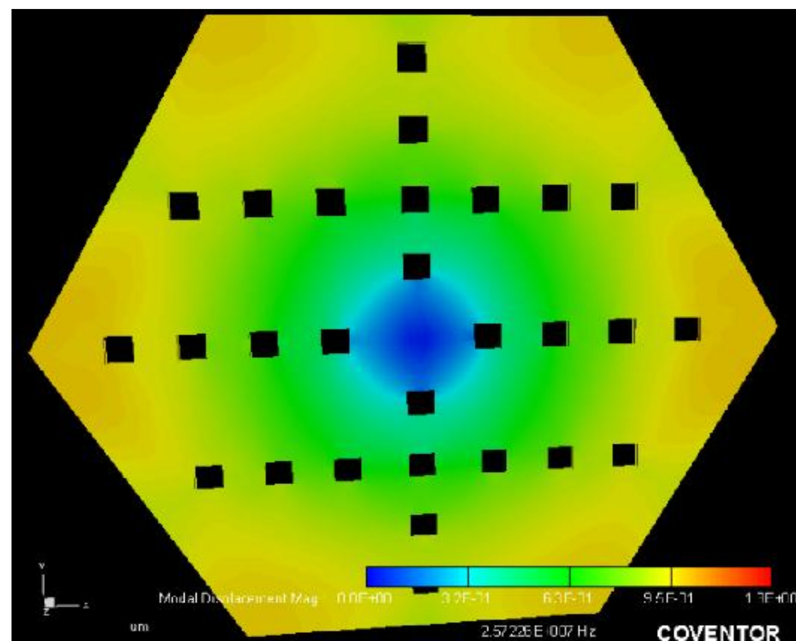

Back

Disk Resonators: Equivalent Model

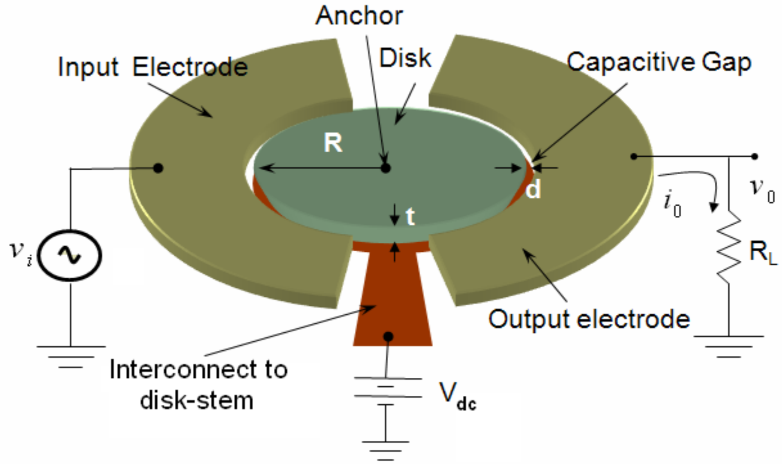

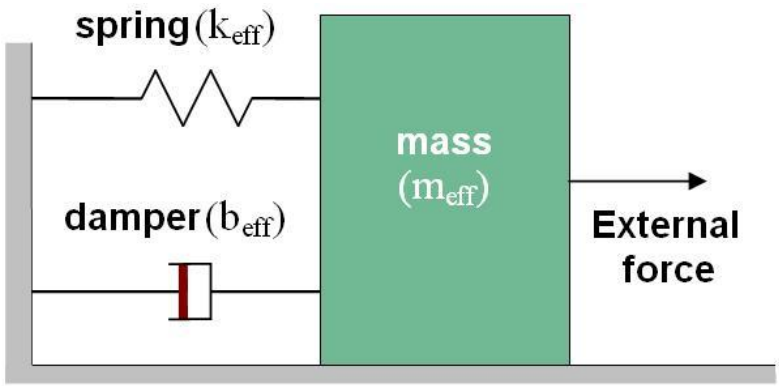

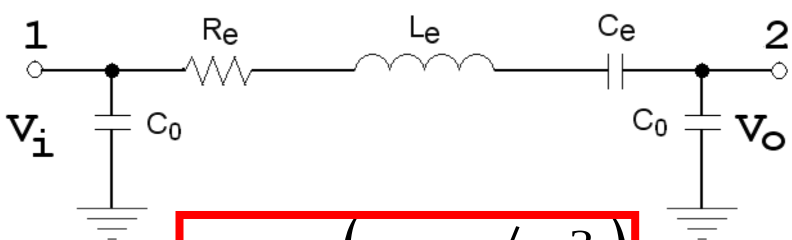

Electrical quantity	Mechanical analog
Voltage (V)	Force (F)
Current (I)	Velocity (v)
Resistance (R)	Damping (b)
Capacitance (C)	Compliance (1/k)
Inductance (L)	Mass (m)

$$L_e = \left(m_{eff} / \eta^2\right)$$

$$R_e = \left(b_{eff} / \eta^2\right)$$

$$C_e = \left(\eta^2 / k_{eff}\right)$$

$$\eta = V_{dc} \frac{\partial C_k}{\partial x}$$

Disk Resonators: Equivalent Model